IFIC Institut de Física Corpuscular
CSIC
Generalitat Valenciana
Conselleria de Educación, Cultura, Universidades y Empleo
Gen—T
Astroparticles
Astroparticles and High Energy Physics Group
Vniversitat de València
Ministerio de Ciencia, Innovación y Universidades
Financiado por la Unión Europea NextGenerationEU
Plan de Recuperación, Transformación y Resiliencia
Agencia Estatal de Investigación

Valentina De Romeri
(IFIC Valencia - UV/CSIC)

COHERENT ELASTIC NEUTRINO-NUCLEUS SCATTERING

2nd EuCAPT Astroneutrino Theory Workshop
IEAP CTU in Prague
16-27 September 2024

A FEW USEFUL REFERENCES

- Papers/Reviews:
  - Coherent elastic neutrino-nucleus scattering: Terrestrial and astrophysical applications M. Abdullah et al.
  - A view of Coherent Elastic Neutrino-Nucleus Scattering, M. Cadeddu, F. Dordei, C. Giunti
  - Recent Probes of Standard and Non-standard Neutrino Physics With Nuclei, Papoulias, Kosmas, Kuno
  - Probing new physics with coherent neutrino scattering off nuclei, Barranco, Miranda, Rashba
  - Walecka and Donnelly https://doi.org/10.1016/0375-9474(76)90209-8

- Dark Matter Direct detection:
  - The Theory of Direct Dark Matter Detection
  - https://arxiv.org/pdf/1904.07915
  - https://arxiv.org/pdf/1002.1912

- Books:
  - Walecka Theoretical Nuclear and Subnuclear Physics, Oxford Stud.Nucl.Phys. 16 (1995) 1-610
  - Giunti & Kim: https://oxford.universitypressscholarship.com/view/10.1093/acprof:oso/9780198508717.001.0001/acprof-9780198508717

- Webpage:
  - http://www.nu.to.infn.it/Neutrino_Lectures

- Magnificent CEvNS workshop talks

OUTLINE

1. Introduction to CEνNS and main features
2. CEνNS physics implications: SM
3. CEνNS physics implications: BSM

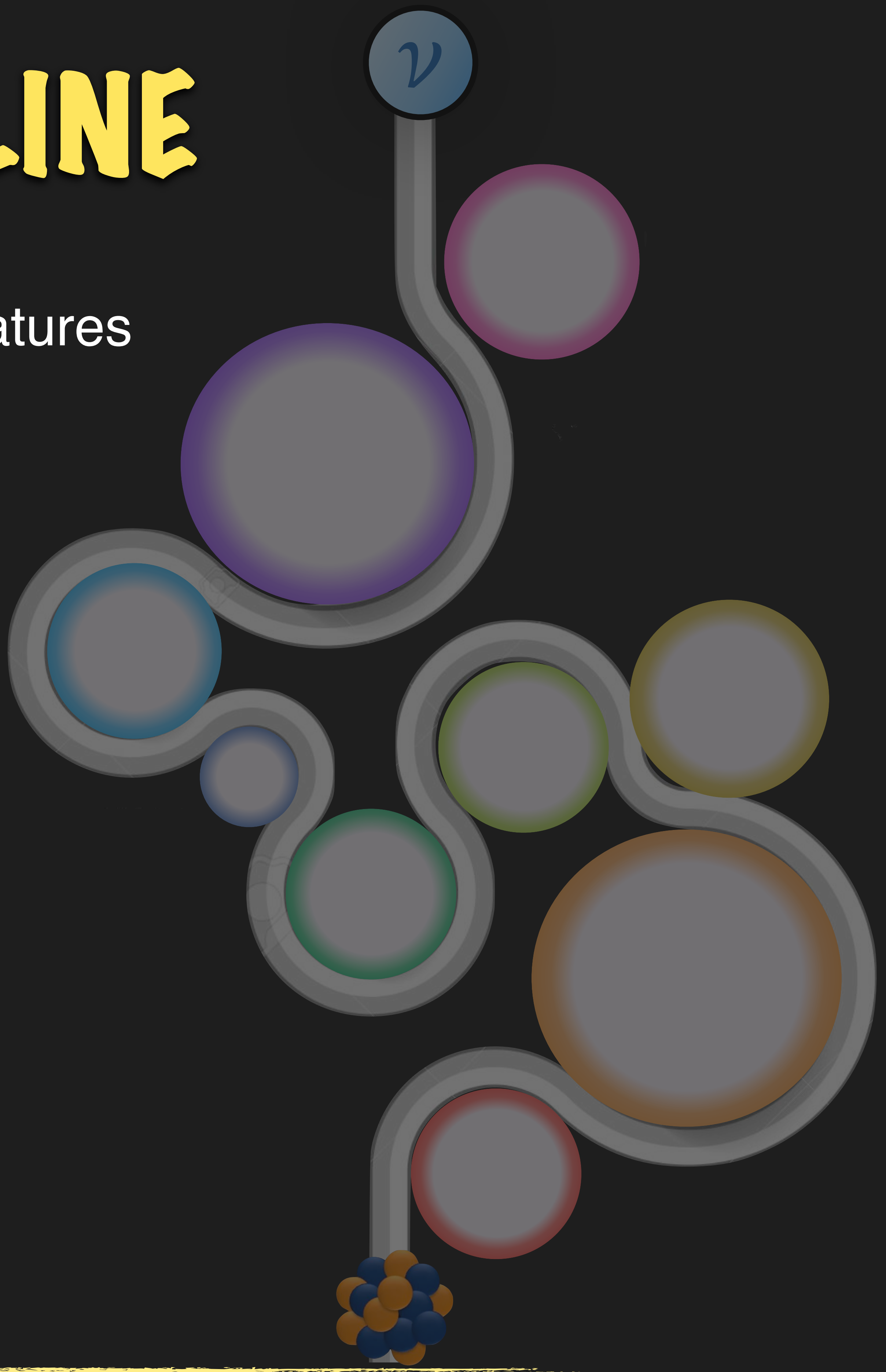

OUTLINE - 1st lecture

- Neutrino interactions with matter, especially nuclei
- CEvNS: introduction and features
- CEvNS: neutrino sources
- CEvNS: experiments and detection
- CEvNS: observations
- CEvNS cross section in the SM

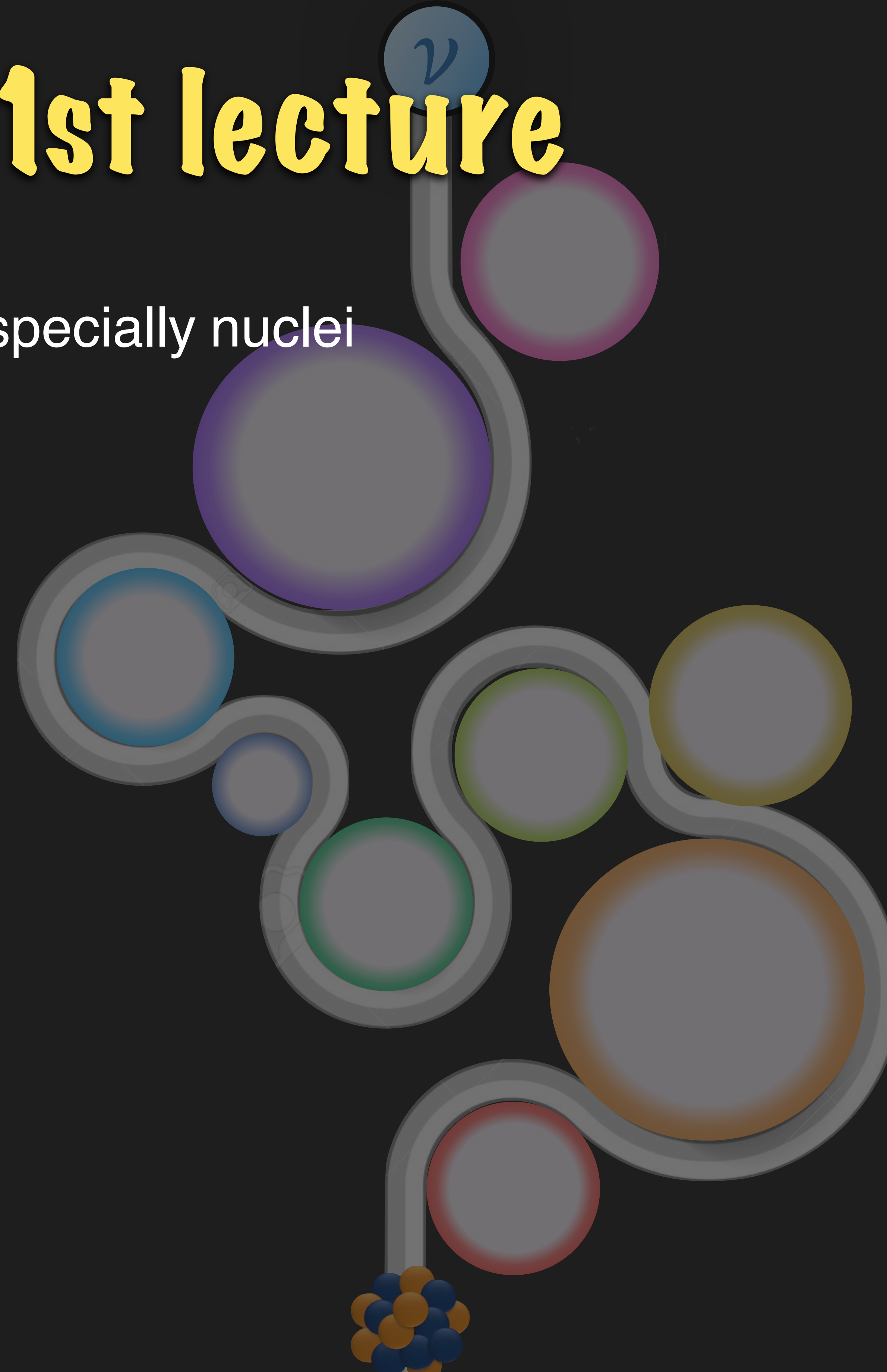

NEUTRINO INTERACTIONS WITH MATTER

Neutrinos are elusive particles but not completely unfriendly

$$\mathcal{L}_{\rm SM} = -\frac{g}{\sqrt{2}} \sum_{\alpha=e,\mu,\tau} \bar{\nu}_{\alpha L}\gamma^{\mu}\ell_{\alpha L}W_{\mu} - \frac{g}{2\cos\theta_{\rm W}} \sum_{\alpha=e,\mu,\tau} \bar{\nu}_{\alpha L}\gamma^{\mu}\ell_{\alpha L}Z_{\mu} + h.c.$$

Charged Current (CC)

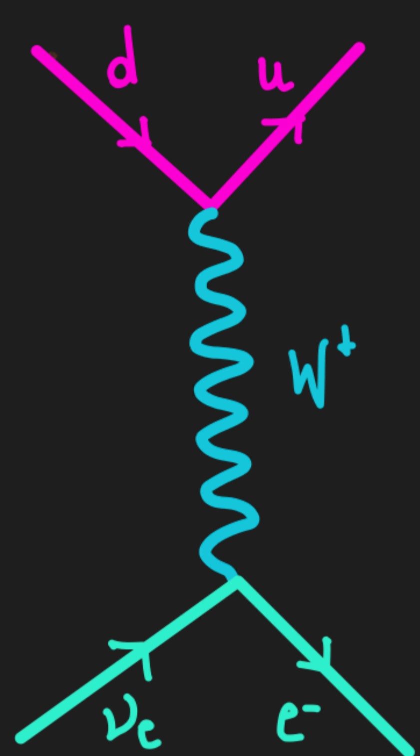

Produces lepton with flavor corresponding to the neutrino flavor

Neutral Current (NC)

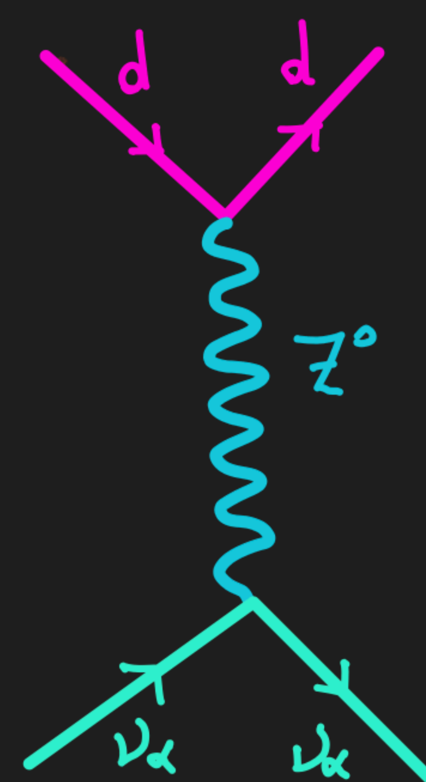

Flavor blind

NEUTRINO INTERACTIONS WITH NUCLEI

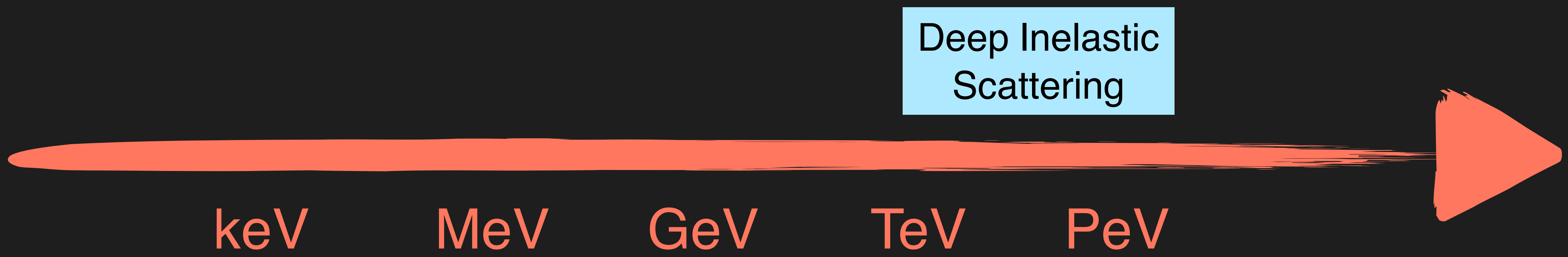

Adapted from Kate Scholberg

NEUTRINO INTERACTIONS WITH NUCLEI

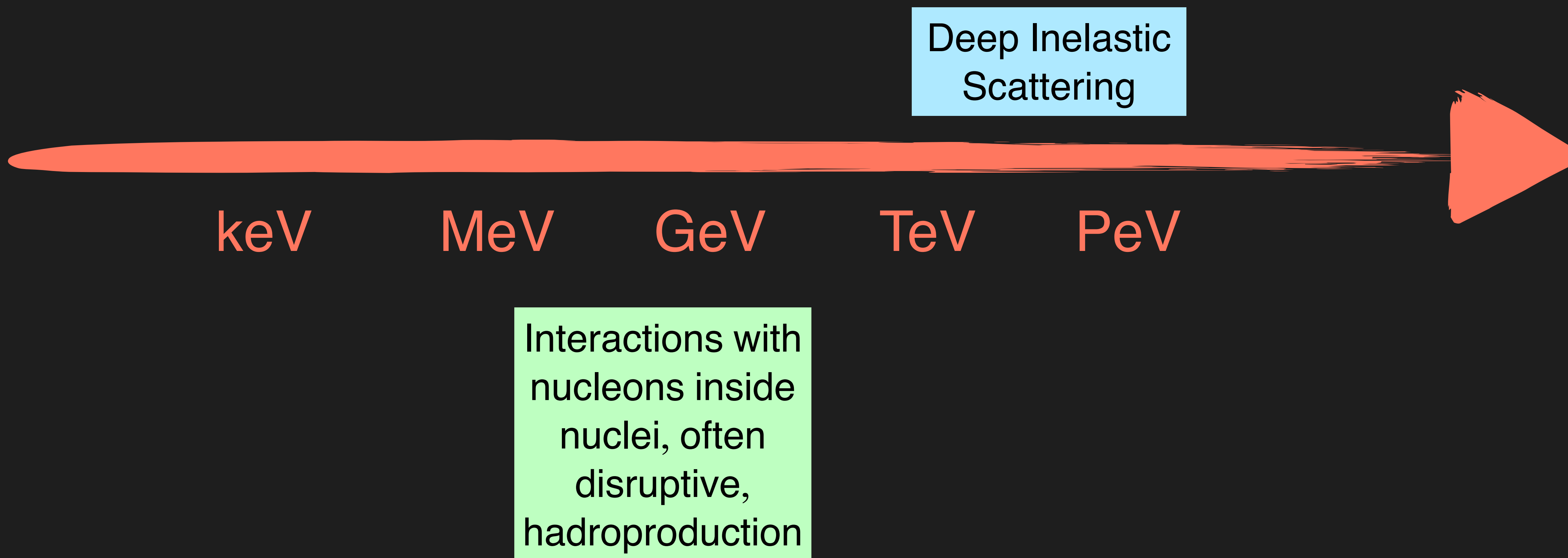

Adapted from Kate Scholberg

NEUTRINO INTERACTIONS WITH NUCLEI

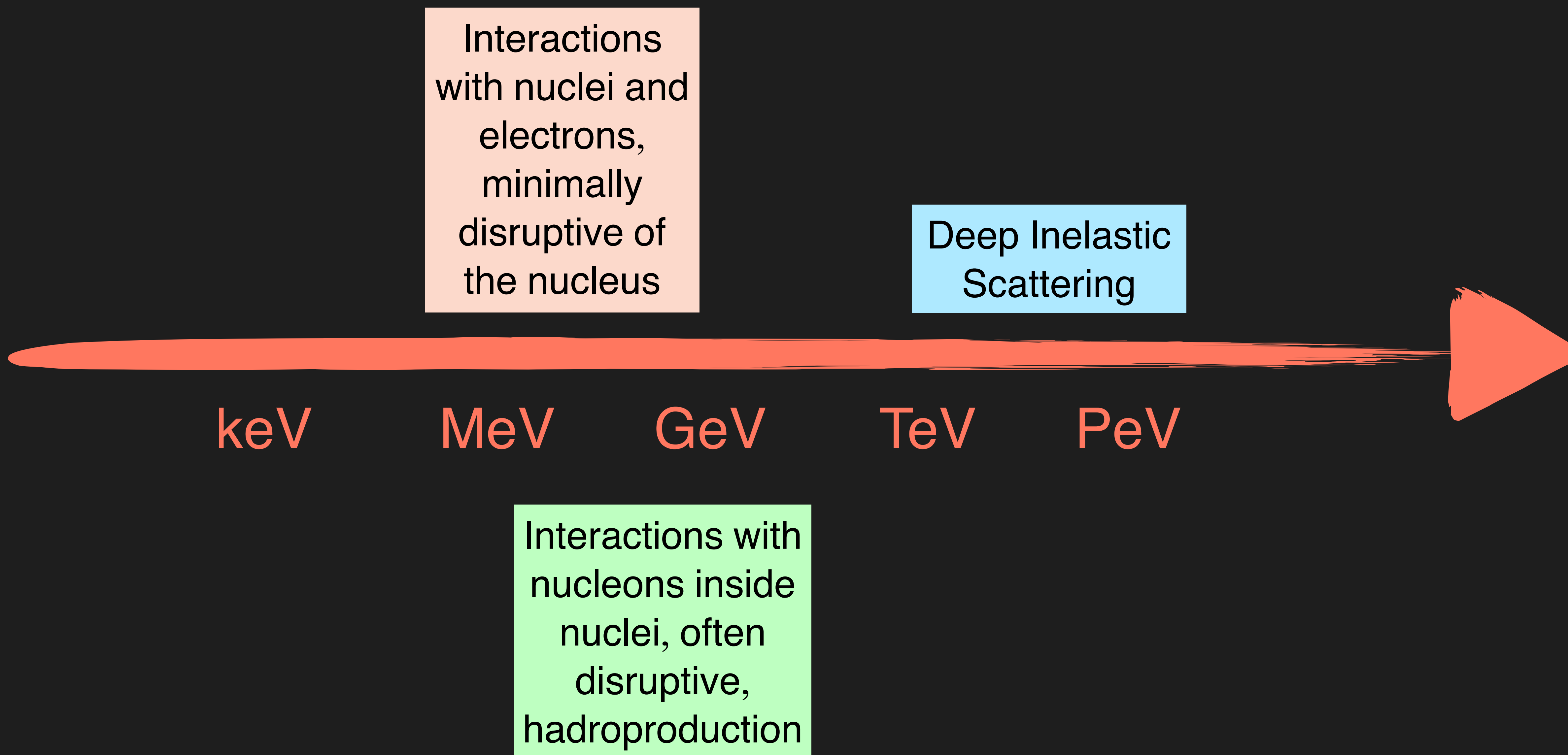

Adapted from Kate Scholberg

NEUTRINO INTERACTIONS WITH NUCLEI

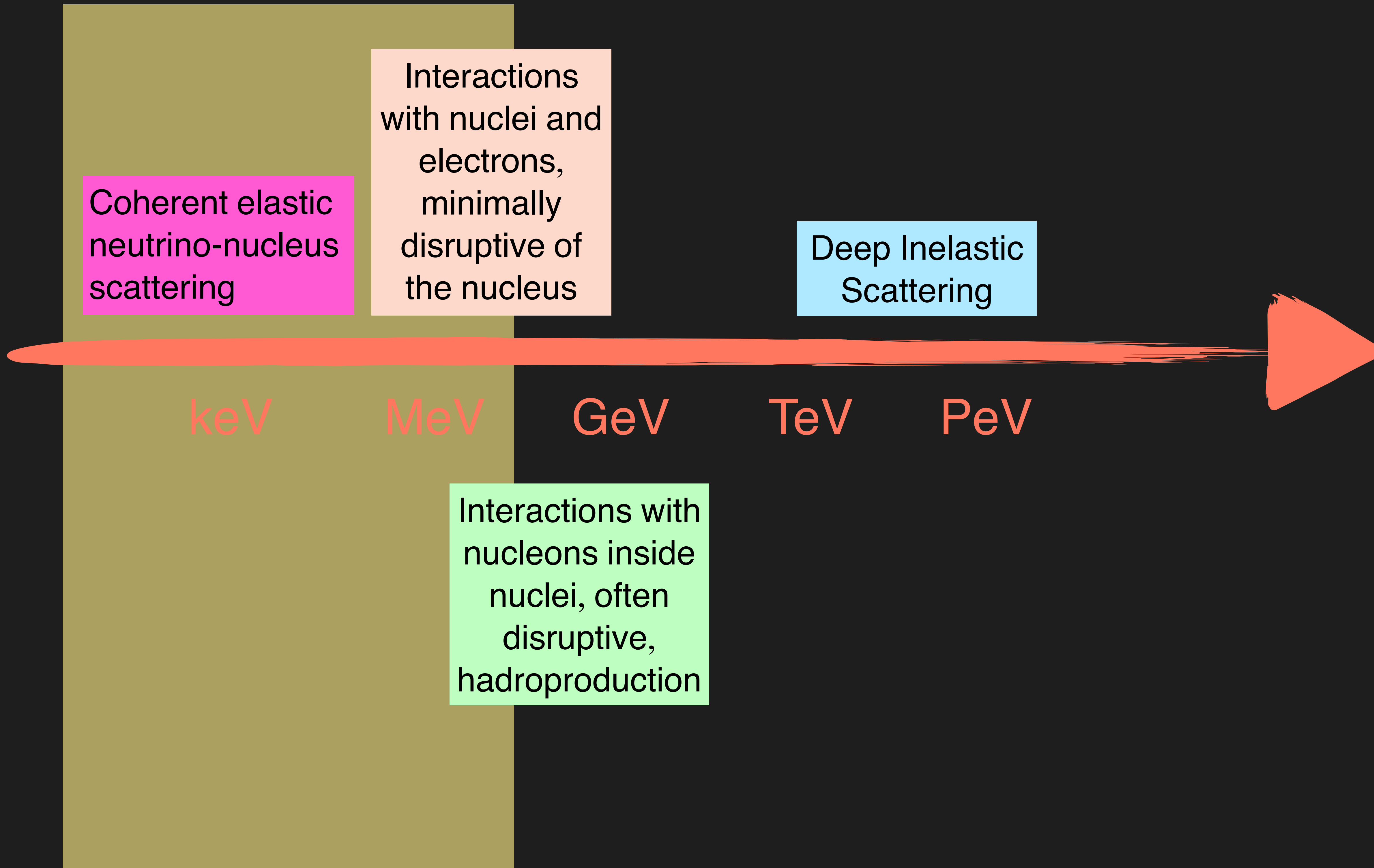

Adapted from Kate Scholberg

CEνNS: INTRODUCTION AND FEATURES

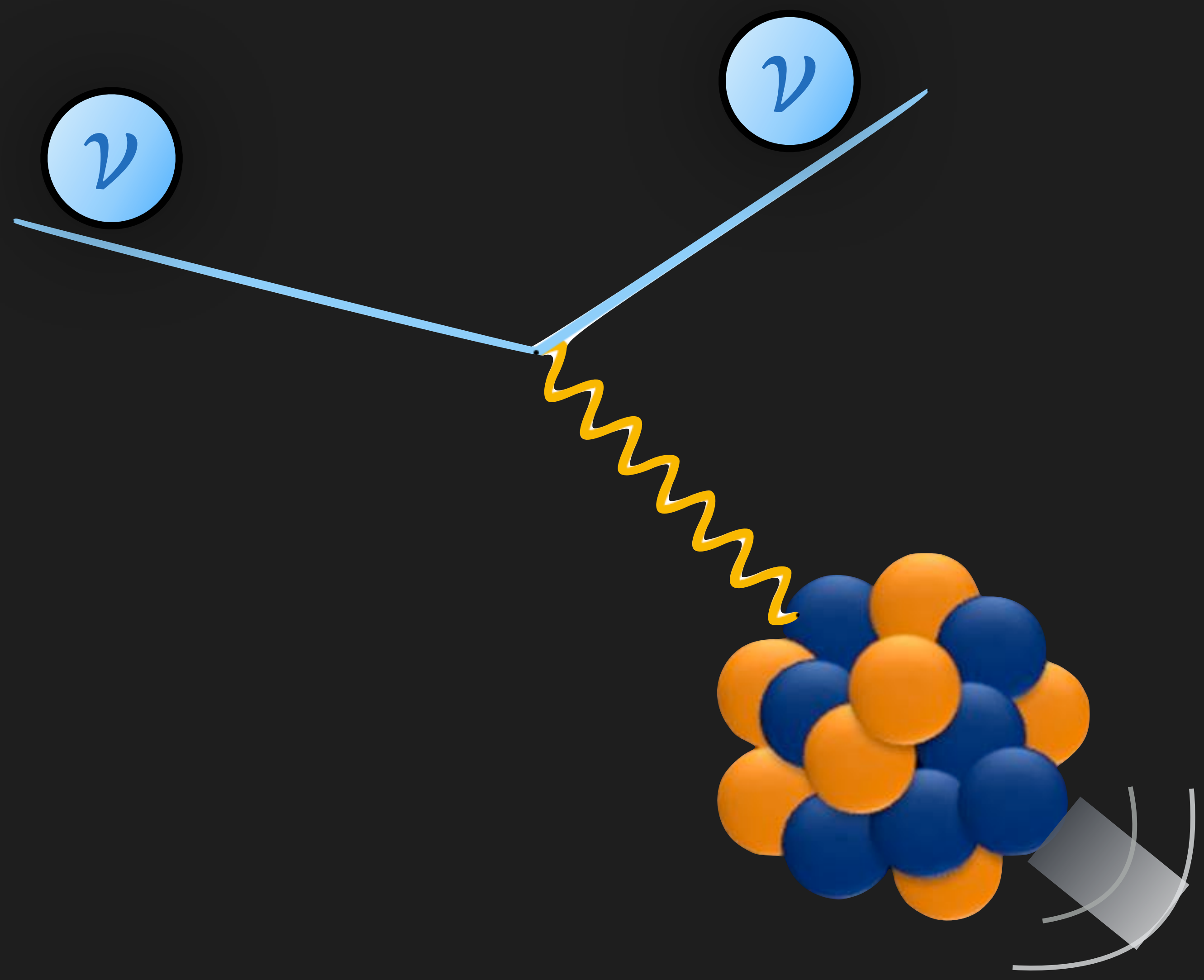

COHERENT ELASTIC NEUTRINO-NUCLEUS SCATTERING (CEνNS)

- Neutral-current process: $\nu + N(A,Z) \rightarrow \nu + N(A,Z)$
- Coherent: target nucleon wave functions remain in phase with each other before and after the collision. Amplitudes of scattering on individual nucleons add
- Elastic: no new particles are created and nuclear target remains in the same energy state
- The neutrino sees the nucleus as a whole:
  => cross section enhancement $\sigma \sim$ (#scatter targets)^2
  => upper limit on neutrino energy (up to $E_\nu \sim 100$ MeV)
- Total cross section scales approximately like N^2

$$\frac{d\sigma}{dE_R} \propto N^2$$

- Can be ~2 orders of magnitude larger than inverse beta decay process used first to observe neutrinos.

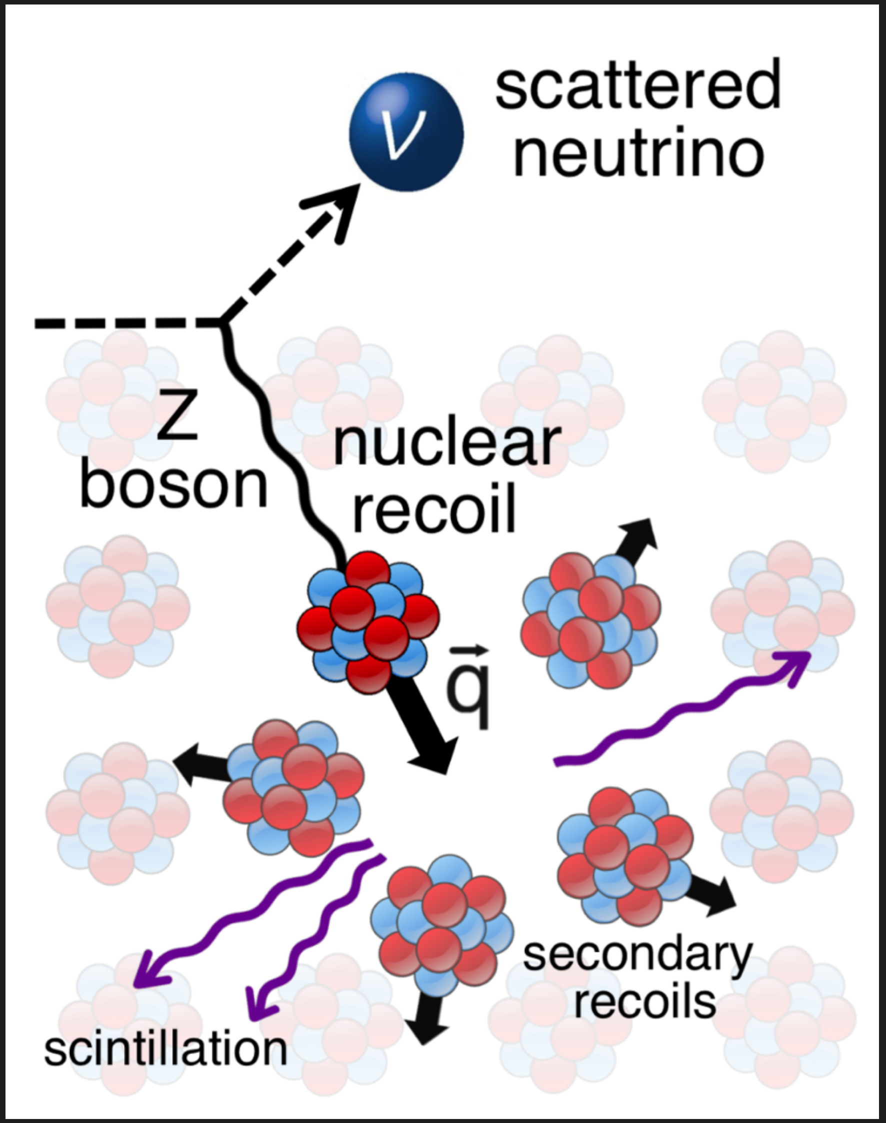

D. Akimov et al, Science 357 (2017)

INCOHERENT/INELASTIC SCATTERING

Incoherent scattering: $\sigma_{\mathrm{NC}}(\nu\mathcal{N}) \propto \sum_i |\mathcal{A}(\nu n_i)|^2 \propto N$ (Probabilities of scattering on individual nucleons add)

Coherent scattering: $\sigma_{\mathrm{NC}}(\nu\mathcal{N}) \propto \left| \sum_i \mathcal{A}(\nu n_i) \right|^2 \propto N^2$ (Amplitudes of scattering on individual nucleons add)

$$\mathcal{A}(\vec{q}) = \sum_{j=1}^{A} a_j(\vec{q}) \exp^{i\vec{q}x_j}$$

When the momentum transfer times the dimension of the nuclear target is very small, qR $\ll 1$, the phase factors are negligible: the amplitude is given by the single constituent amplitude multiplied by the constituents number A.

Bednyakov and Naumov Phys. Rev. D 98 no. 5, (2018) 053004
Pirinen+ Adv. High Energy Phys. 2018 (2018) 9163586,
Bednyakov and Naumov Phys. Part. Nucl. Lett. 16 no. 6, (2019) 638-646

INCOHERENT/INELASTIC SCATTERING

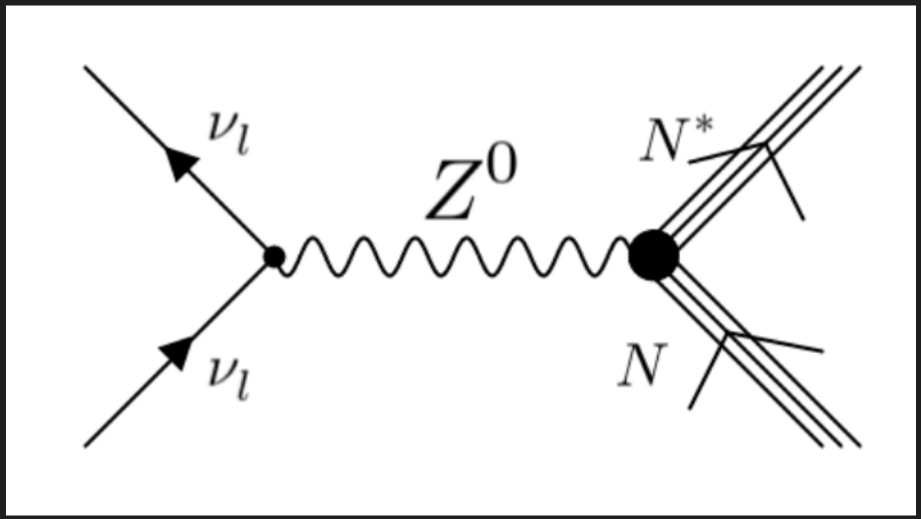

Neutrinos with energies of tens of MeV can excite many states in the target nuclei used for CEvNS experiments.

This cross-section has a linear dependence on the number of nucleons.

Going to higher neutrino energies, an approximation hints towards a smooth transition between the coherent and incoherent neutrino-nucleus scattering regime.

A correct treatment of both channels requires an accurate evaluation of the transition matrix elements describing the various interaction channels between the initial and final nuclear states.

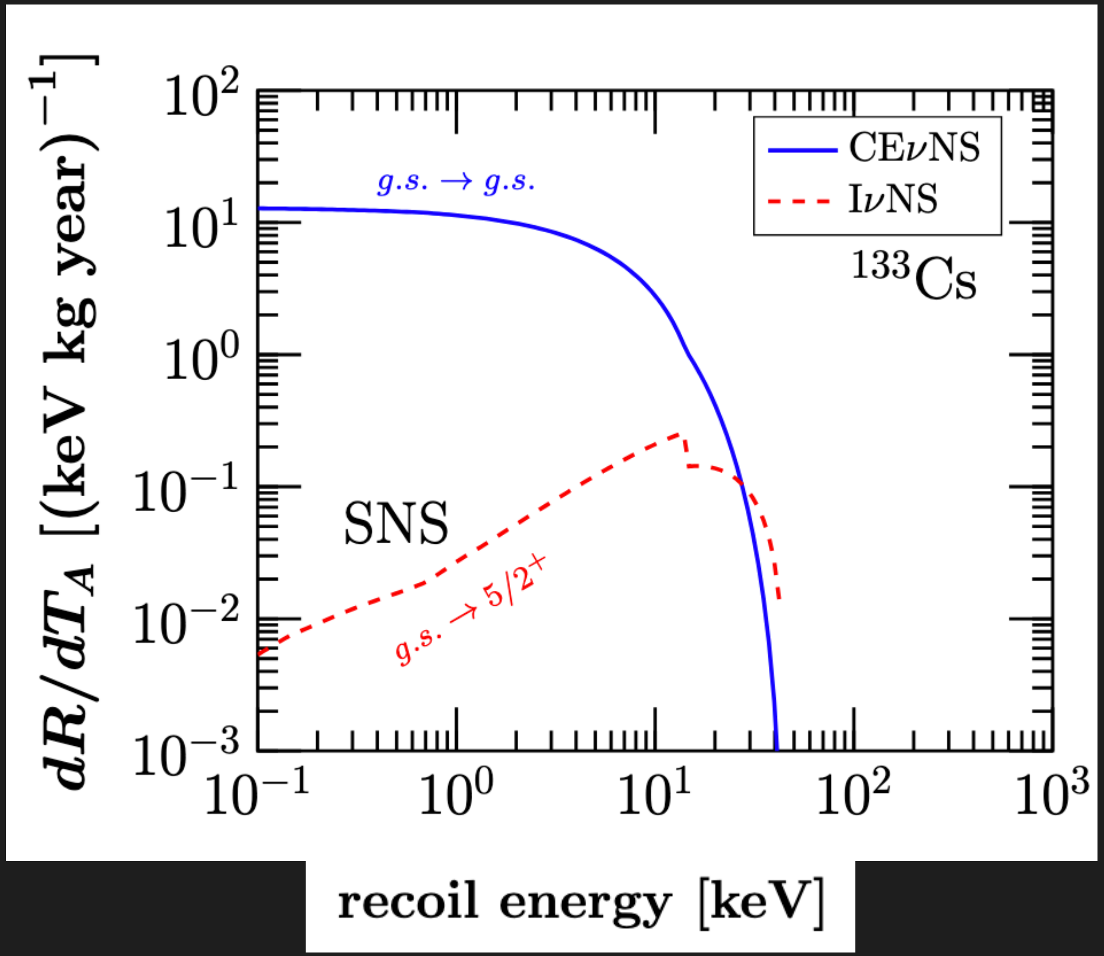

Sahu+ Phys. Rev. C. 102 035501
Bednyakov+ Phys. Rev. D 98 (2018) 053004
Dutta+ Phys. Rev. D 106, 113006 (2022)
...

Sahu+ Phys. Rev. C. 102 035501

AN ACT OF HUBRIS

First theoretically predicted in 1974

D.Z. Freedman, Phys. Rev. D 9 (1974)
V.B. Kopeliovich and L.L. Frankfurt, JETP Lett. 19 4 236 (1974)

PHYSICAL REVIEW D VOLUME 9, NUMBER 5 1 MARCH 1974

Coherent effects of a weak neutral current

Daniel Z. Freedman†
National Accelerator Laboratory, Batavia, Illinois 60510
and Institute for Theoretical Physics, State University of New York, Stony Brook, New York 11790
(Received 15 October 1973; revised manuscript received 19 November 1973)

If there is a weak neutral current, then the elastic scattering process $\nu + A \to \nu + A$ should have a sharp coherent forward peak just as $e + A \to e + A$ does. Experiments to observe this peak can give important information on the isospin structure of the neutral current. The experiments are very difficult, although the estimated cross sections (about 10^{-38} cm^2 on carbon) are favorable. The coherent cross sections (in contrast to incoherent) are almost energy-independent. Therefore, energies as low as 100 MeV may be suitable. Quasi-coherent nuclear excitation processes $\nu + A \to \nu + A^*$ provide possible tests of the conservation of the weak neutral current. Because of strong coherent effects at very low energies, the nuclear elastic scattering process may be important in inhibiting cooling by neutrino emission in stellar collapse and neutron stars.

Our suggestion may be an act of hubris, because the inevitable constraints of interaction rate, resolution, and background pose grave experimental difficulties for elastic neutrino-nucleus scattering. We will discuss these problems at the end of this note, but first we wish to present the theoretical ideas relevant to the experiments.

Experimentally the most conspicuous and most difficult feature of our process is that the only detectable reaction product is a recoil nucleus of low momentum. Ideally the apparatus should have sufficient resolution to identify and determine the momentum of the recoil nucleus and sufficient mass to achieve a reasonable interaction rate. Neutron background is a serious problem

CEνNS was observed for the first time ~40 years later,
in 2017 by the COHERENT experiment at the Oak Ridge Spallation Neutron Source.

COHERENT ELASTIC NEUTRINO-NUCLEUS SCATTERING

CEνNS is an exceptionally challenging process to observe

Despite its large cross section, not observed for years due to tiny nuclear recoil energies

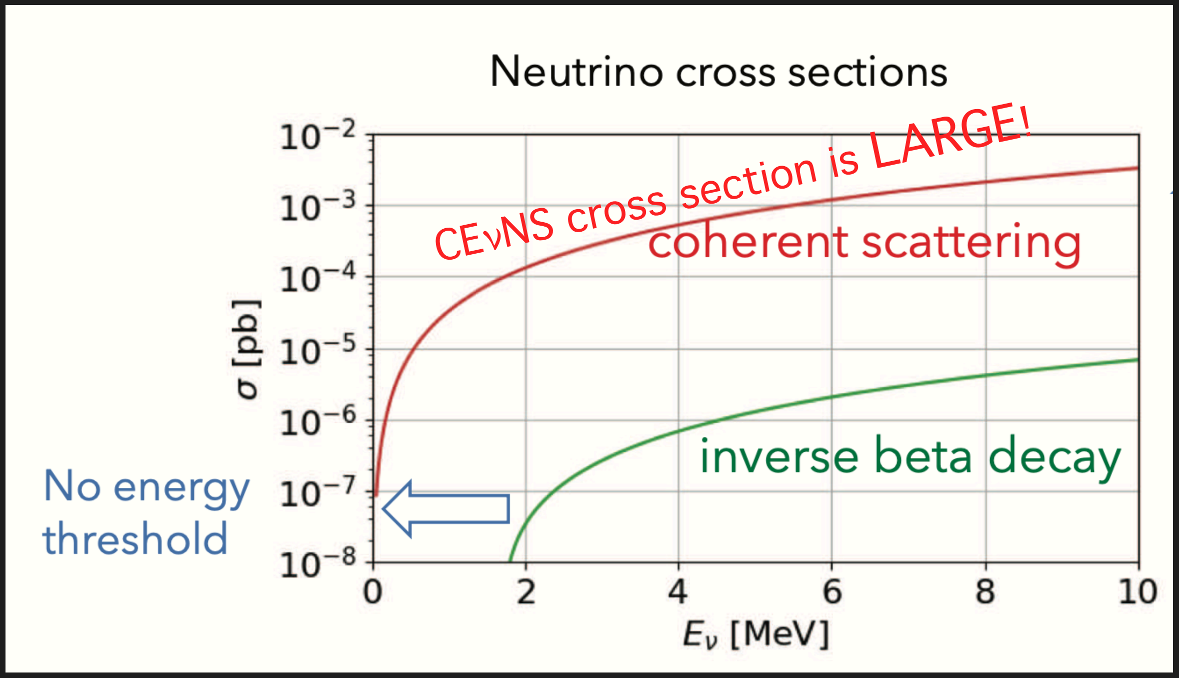

Credit: R. Strauss @ Magnificent CEvNS

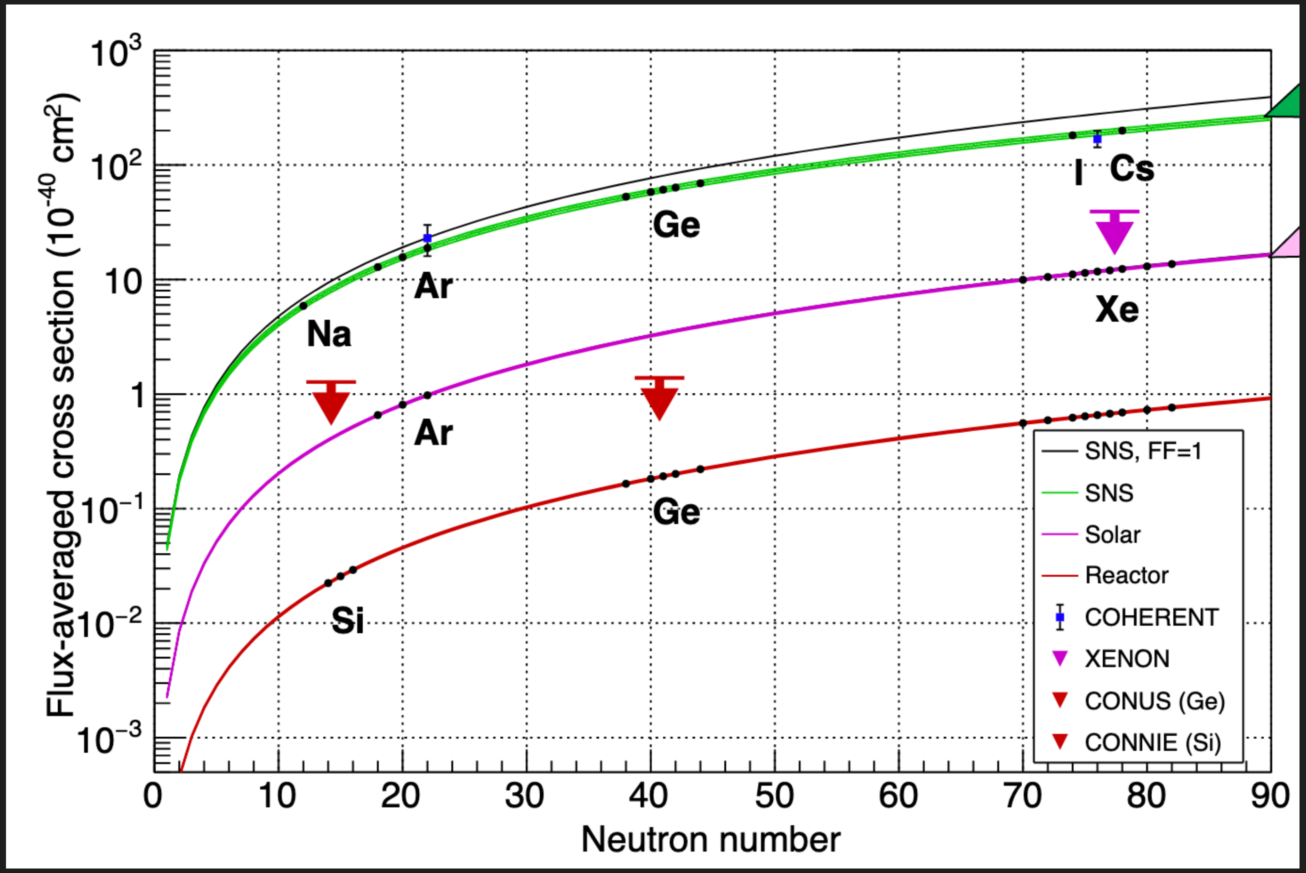

Credit to K. Scholberg @ISAPP 2021

NEUTRINO-NUCLEUS SCATTERING

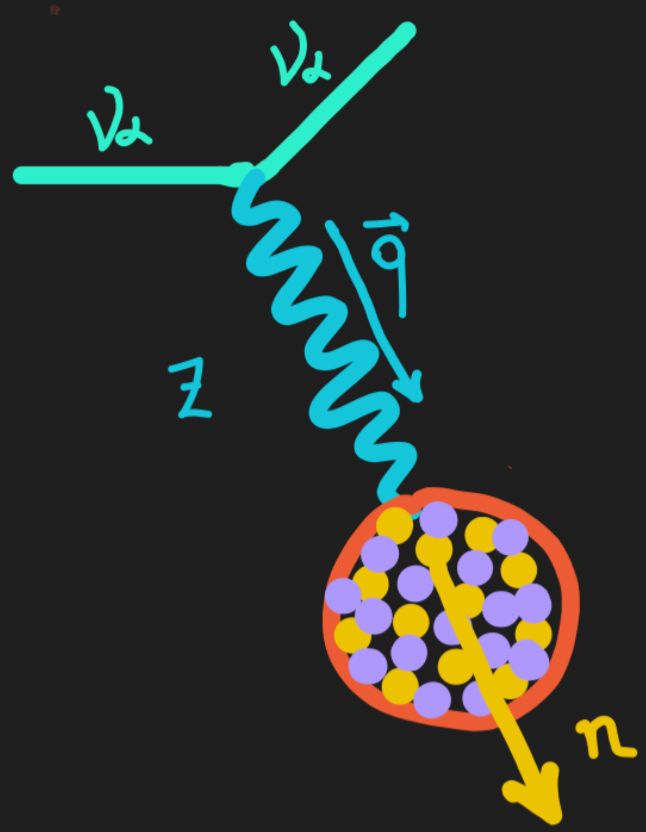

Inelastic incoherent

$\lambda_Z \ll 2R$

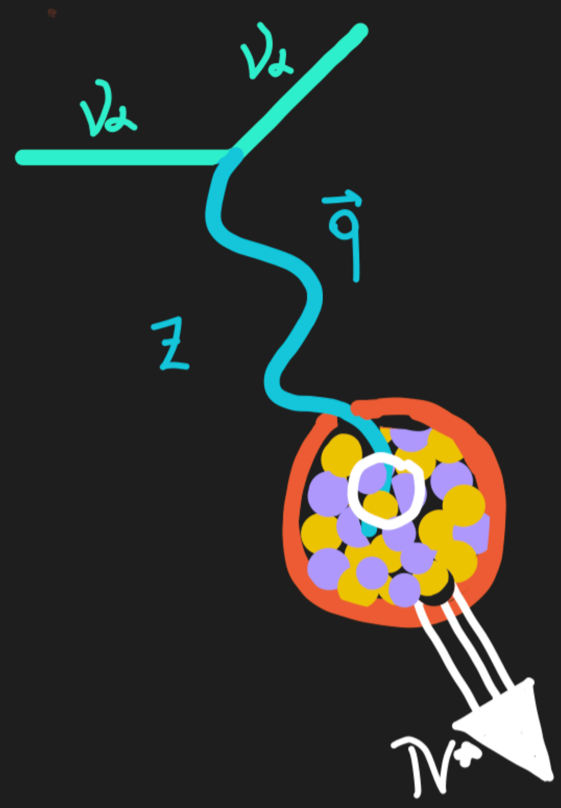

Elastic incoherent

$\lambda_Z \lesssim 2R$

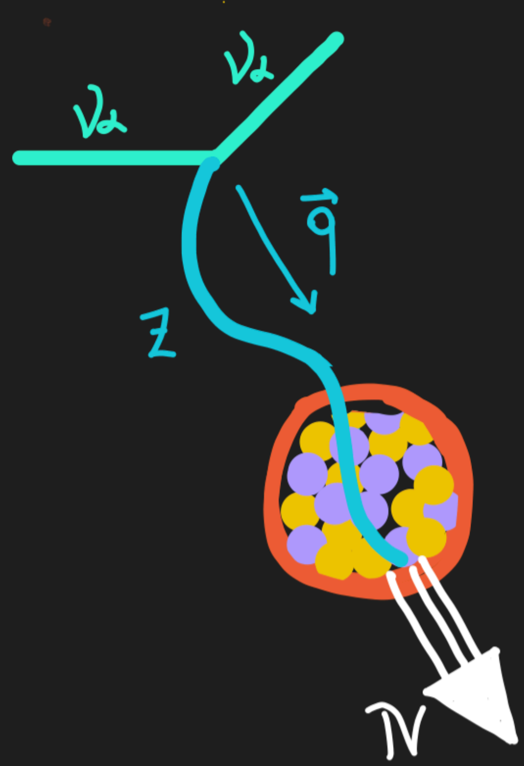

Elastic coherent

$\lambda_Z \gtrsim 2R$ (Natural units!)

$$\lambda_Z = 2\pi \frac{\hbar}{|\vec{q}|}$$

Different types of interactions of a neutrino ν_α with a nucleus, depending on the wavelength of the mediator.

Adapted from Carlo Giunti

NEUTRINO-NUCLEUS SCATTERING

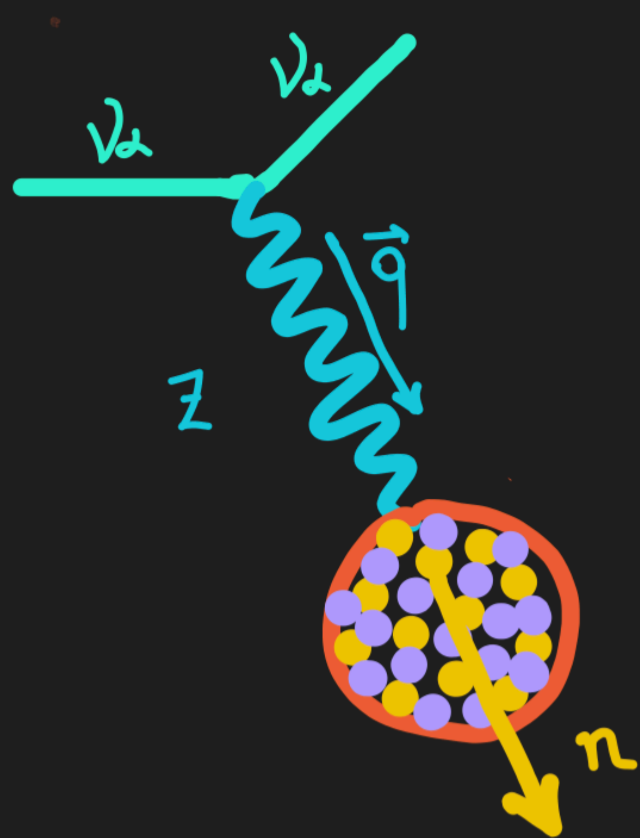

Inelastic incoherent
$\lambda_Z \ll 2R$

When $\lambda_Z \ll 2R$ the Z boson has a high probability of interacting with a single nucleon in the nucleus, ejecting it.

$$\lambda_Z = 2\pi \frac{\hbar}{|\vec{q}\,|}$$

NEUTRINO-NUCLEUS SCATTERING

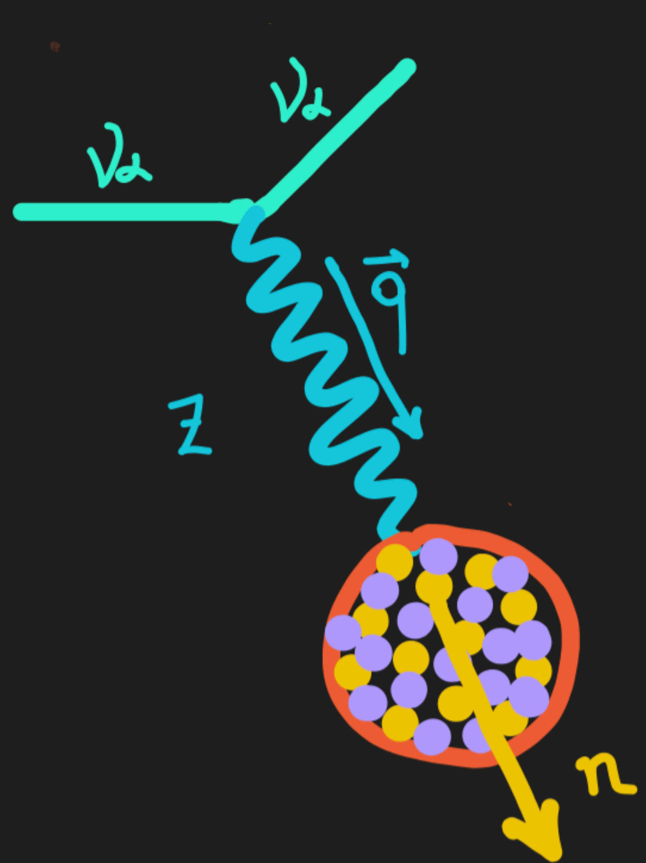

Inelastic incoherent
$\lambda_Z \ll 2R$

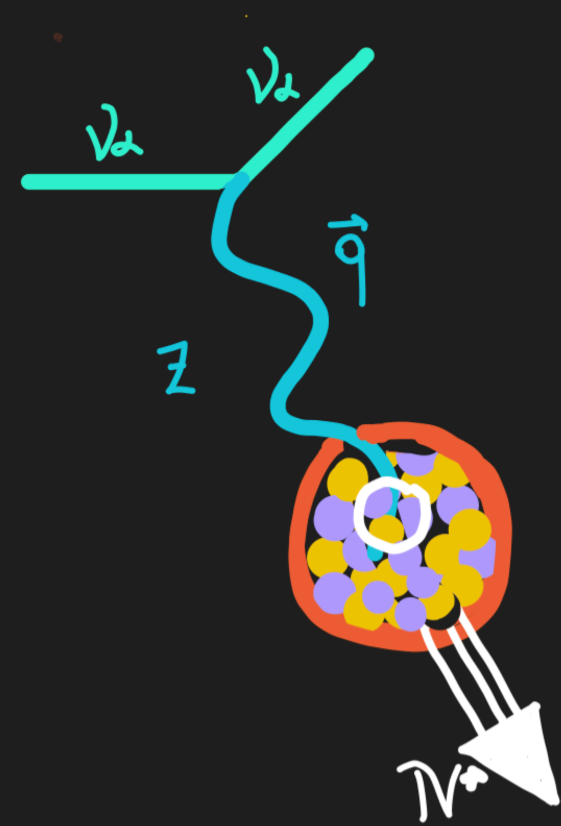

Elastic incoherent
$\lambda_Z \lesssim 2R$

When $\lambda_Z \lesssim 2R$ the Z boson has a high probability of interacting with a group of nucleons inside the nucleus, exciting the latter to the state N*.

$$\lambda_Z = 2\pi \frac{\hbar}{|\vec{q}|}$$

NEUTRINO-NUCLEUS SCATTERING

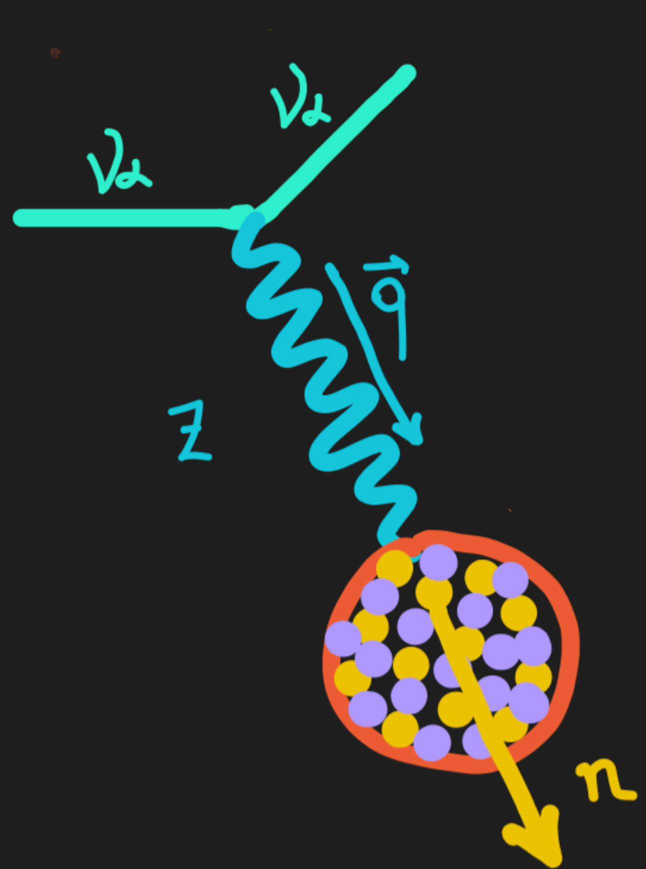

Inelastic incoherent

$\lambda_Z \ll 2R$

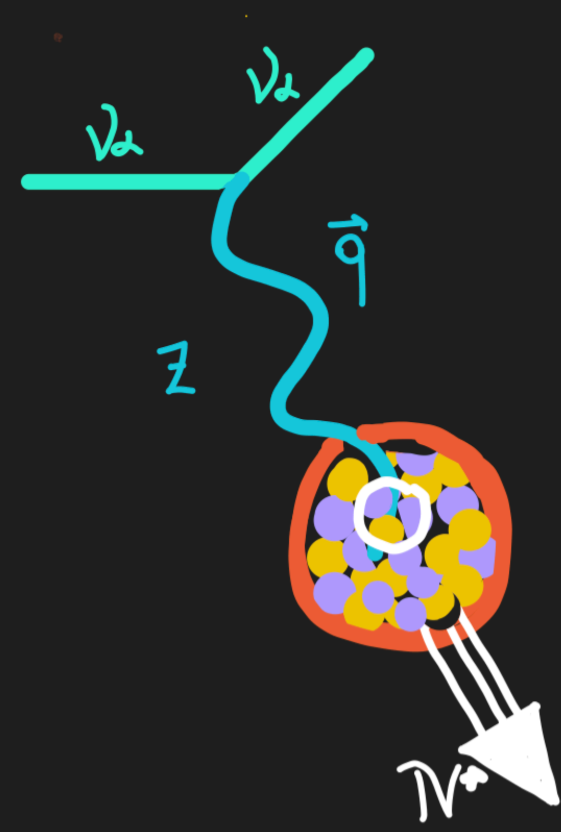

Elastic incoherent

$\lambda_Z \lesssim 2R$

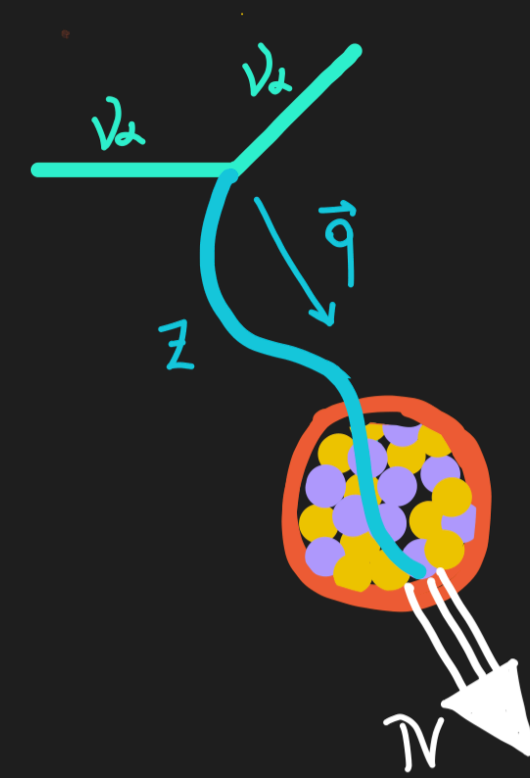

Elastic coherent

$\lambda_Z \gtrsim 2R$

$$\lambda_Z = 2\pi \frac{\hbar}{|\vec{q}\,|}$$

CEνNS occurs when the neutrino energy E_ν is such that amplitudes sum up coherently: $|\vec{q}| \lesssim 1/R_{\text{nucleus}}$ (Natural units!)

COHERENT ELASTIC NEUTRINO-NUCLEUS SCATTERING

Heavy target nucleus:

A = 133, M ~ 133 GeV
R = 1.2 $A^{1/3}$ ~ 6 fm

CEνNS occurs for $|\vec{q}| \lesssim 35$ MeV

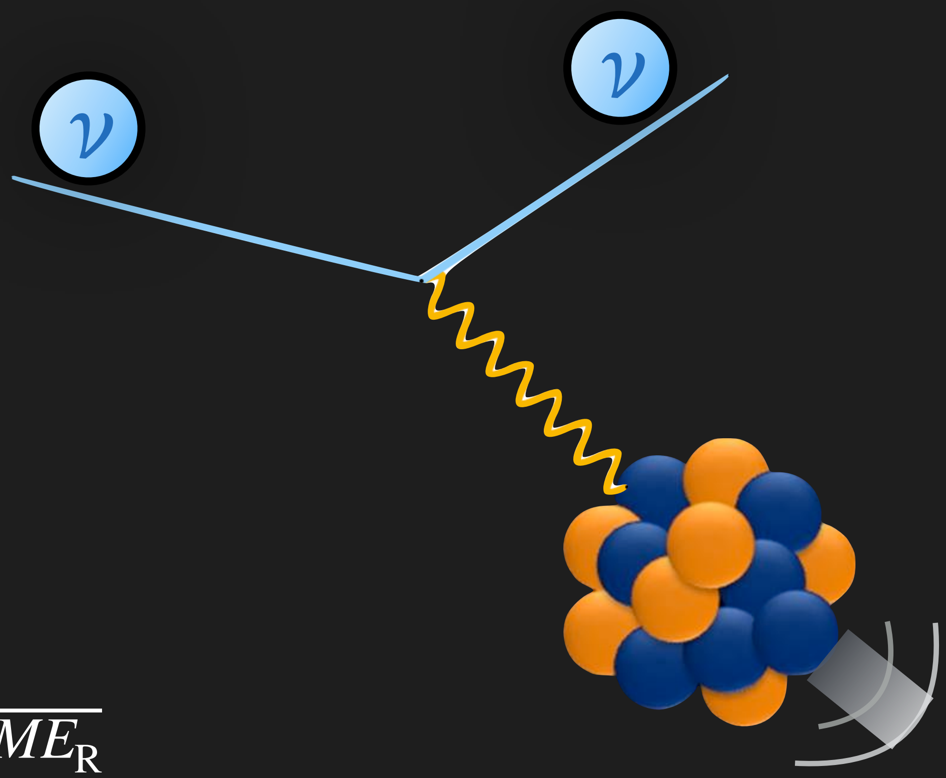

Non-relativistic nuclear recoil: $|\vec{q}| \sim \sqrt{2ME_R}$

COHERENT ELASTIC NEUTRINO-NUCLEUS SCATTERING

Maximum nuclear recoil is $E_R^{\max} = \frac{2E_\nu^2}{m_N}$

Accelerator neutrinos: $E_\nu \lesssim 50\ \mathrm{MeV}$ $E_R \lesssim \mathcal{O}(10)\ \mathrm{keV}$

Close to decoherence

Reactor neutrinos: $E_\nu \lesssim 10\ \mathrm{MeV}$ $E_R \lesssim \mathcal{O}(100)\ \mathrm{eV}$

Full coherence

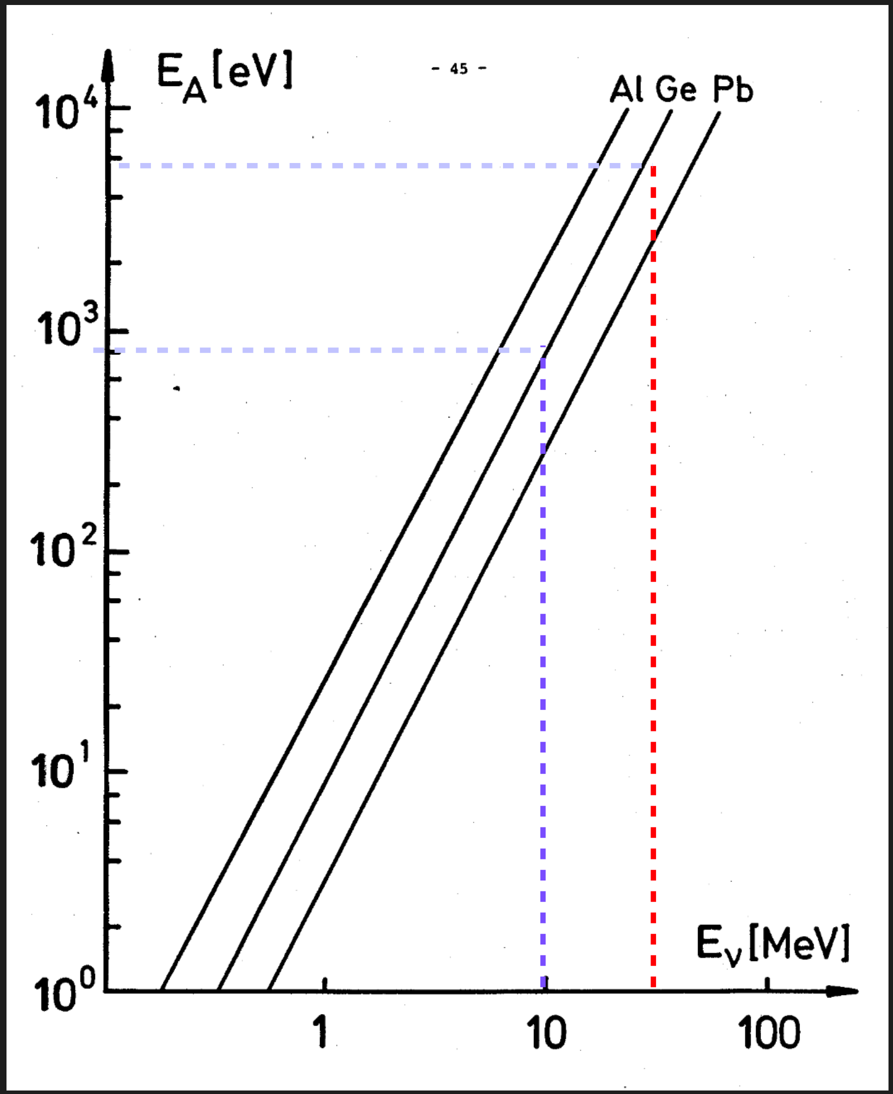

Drukier, Stodolsky, PRD 30 (1984) 2295

- No threshold
- Heavier nuclei: higher cross section but lower recoil
- Both cross-section and maximum recoil energy increase with neutrino energy

BONUS SLIDE. WHAT HAPPENS AT EVEN LOWER E_R?

The de Broglie wavelength of particles scales inversely with their momentum: $\lambda_{\rm DB} \sim \frac{1}{p}$.

Particles scattering with lower momentum see a larger target and scatter with larger cross sections.

BONUS SLIDE. WHAT HAPPENS AT EVEN LOWER E_R?

If $|\vec{q}| \leq 1/R_{atom}$ the reaction occurs with the whole atom.

Coherence would be visible for $|\vec{q}| \sim \mathbf{2\ keV}/R_{atom}$ with a corresponding recoil energy

$$E_R \approx 2\text{meV}/(AR^2_{\text{atom}}[\text{Å}])$$

For Helium, $R_{\text{atom}} = 0.5\text{Å}$ and $E_R \sim 2$ meV.

Sehgal+ Phys.Lett.B 171 (1986) 107-112
Cadeddu+ Phys. Rev. D 100, 073014 (2019)
Donchenko+ FIELDS, PARTICLES, AND NUCLEI 117 (2023)

Electrons “screen" the nuclear weak charge as seen by an electron neutrino (destructive interference).

Observation requires:

- Sensitivity to tiny recoil energies
- neutrinos with energy of few keV

BONUS SLIDE. WHAT HAPPENS AT EVEN LOWER E_R?

Observing relic neutrinos?

Relic neutrinos have momenta p ~ 0.5 meV, corresponding to macroscopic wavelengths $\lambda \sim$ mm and an enhancement factor of order the Avogadro number.

Opher, Astron. Astrophys. 37 (1974) no.1, 135-137
Lewis, PRD 21 (1980), 663
Shvartsman+, JETP Lett. 36 (1982), 277-279
Smith and Lewin, PLB 127 (1983), 185-190
Duda+ PRD 64 (2001), 122001
Domcke and Spinrath, JCAP 06 (2017), 055
Shergold JCAP 11 (2021), 052
...

CEνNS EXPERIMENTS AND DETECTION

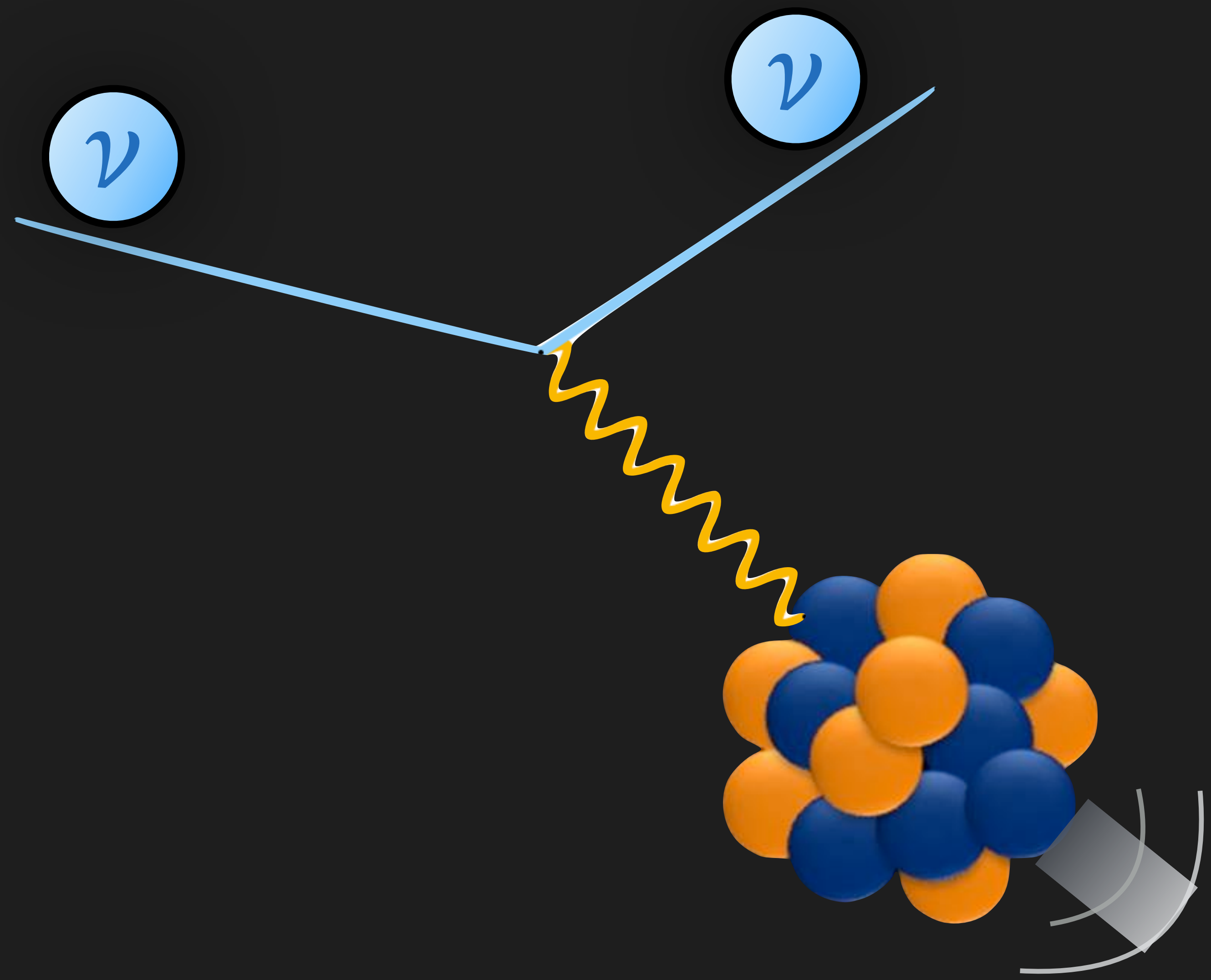

NEUTRINO SOURCES

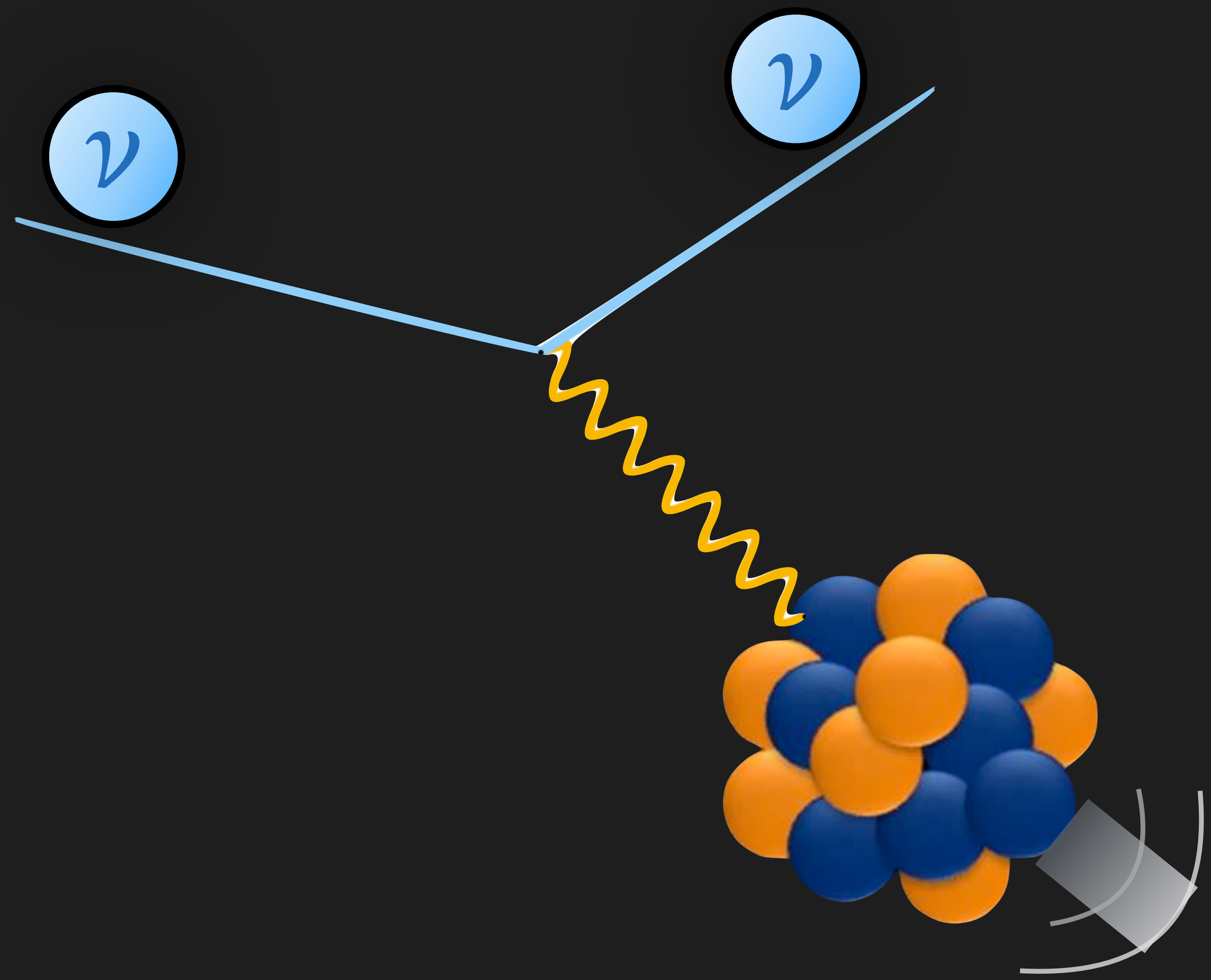

NEUTRINO SOURCES

Preferable requisites:

- High flux
- Well understood spectrum
- Multiple flavours
- Possibility of locating the detector close to the source
- Background rejection

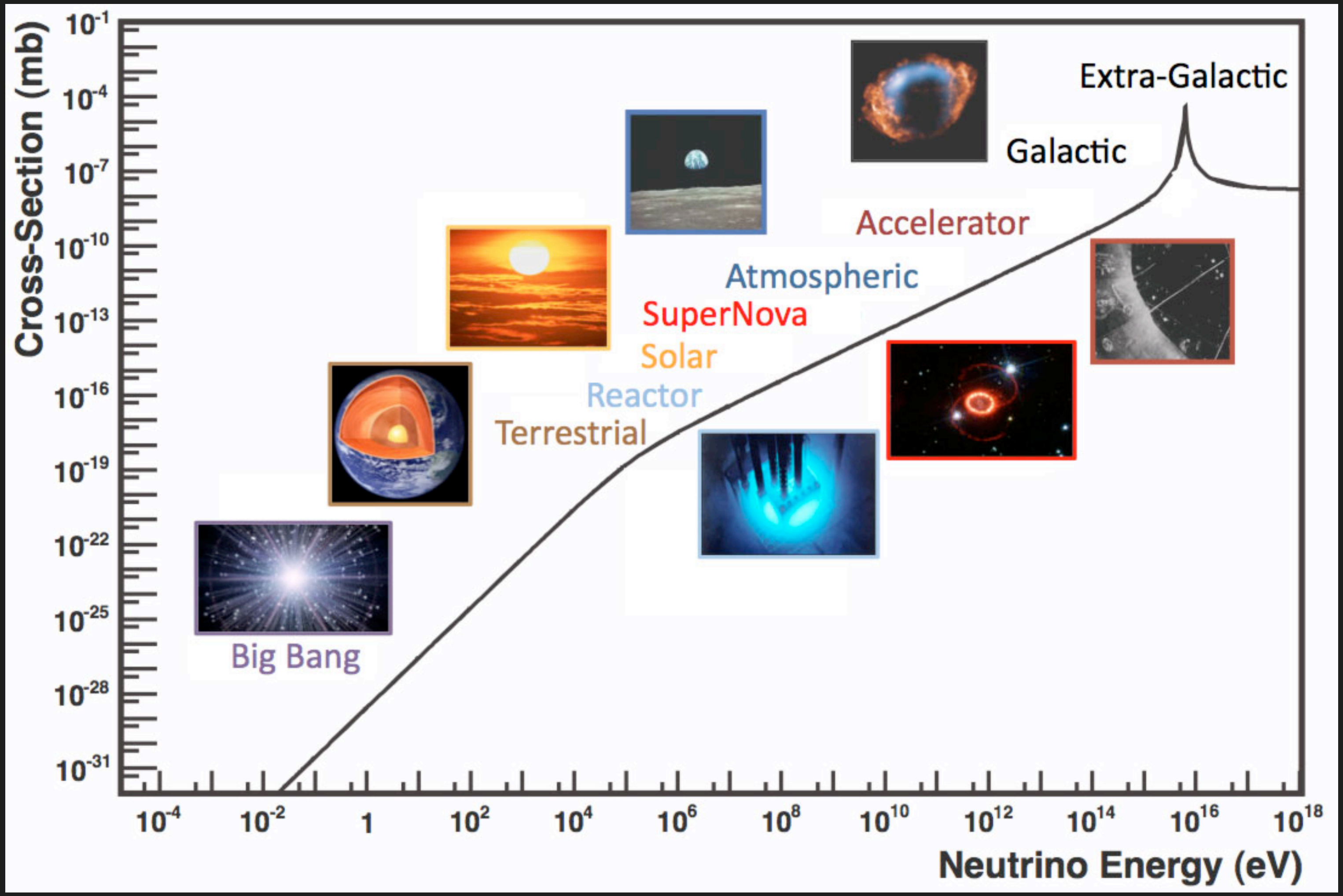

Rev.Mod.Phys. 84 (2012) 1307-1341

LOW-ENERGY NEUTRINOS FROM NATURAL SOURCES

Supernova bursts neutrinos

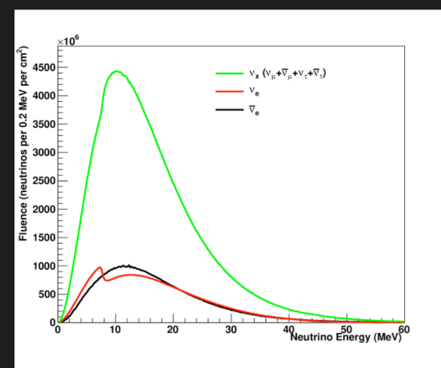

arXiv:1205.6003 [astro-ph.IM]

Atmospheric neutrinos

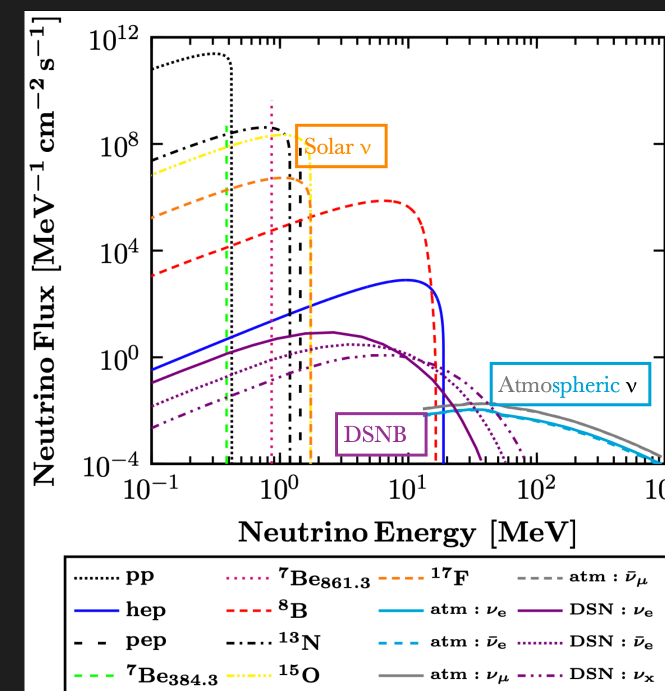

Aristizabal, VDR, Flores, Papoulias JCAP 01 (2022) 01, 055

Solar neutrinos

DSNB

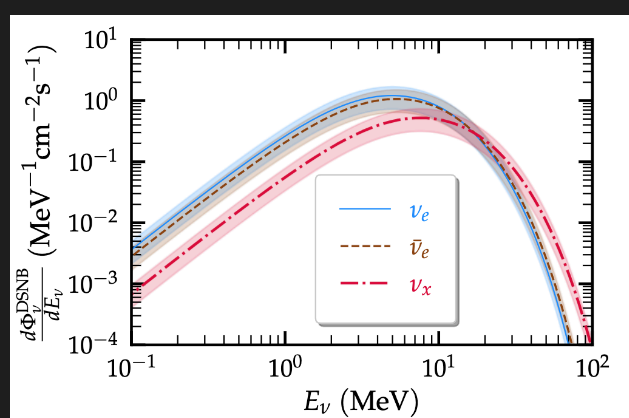

VDR, Majumdar+ 2309.04117 [hep-ph]

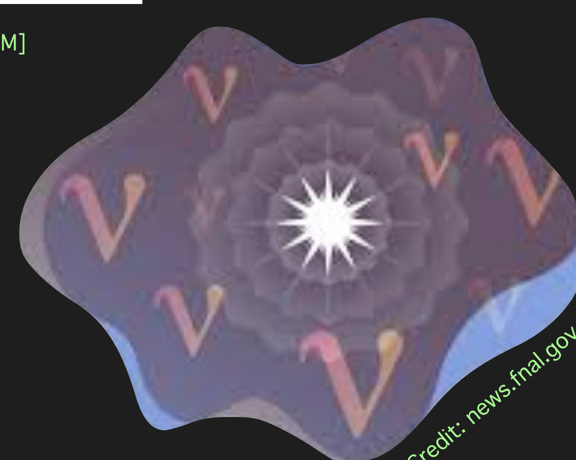

Credit: news.fnal.gov

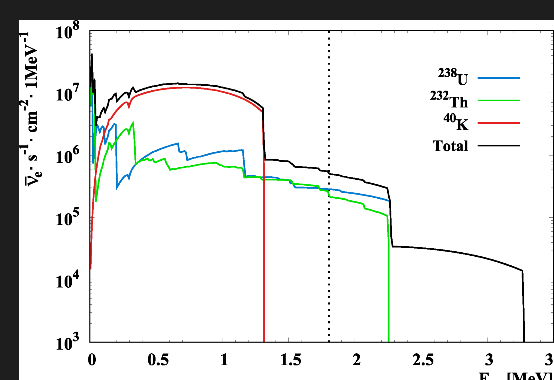

Phys. Rev. D 101, 012009

Geoneutrinos

LOW-ENERGY NEUTRINOS FROM ARTIFICAL SOURCES

Radioactive source ^{51}Cr

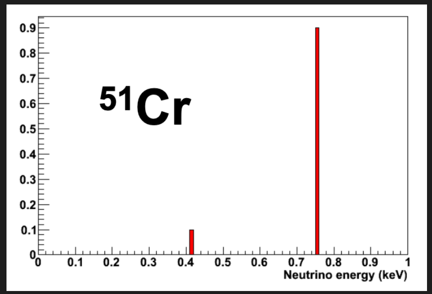

Electron-capture decaying isotope
4 monochromatic lines
very short baseline
low energy challenging

Stopped pions (Decay at rest)

High energy, pulsed beam

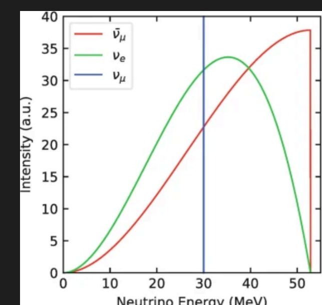

Scolz, https://doi.org/10.1007/978-3-319-99747-6_3

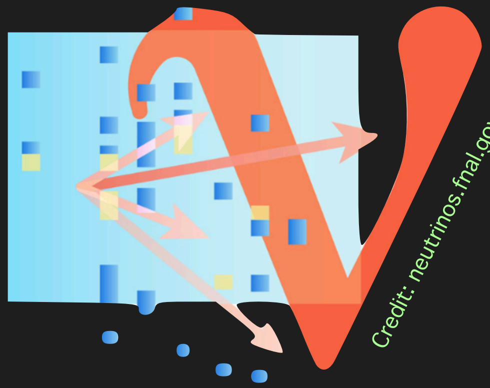

Credit: neutrinos.fnal.gov

Beam induced radioactive sources (IsoDAR)

Higher energy than reactors
Does not exist yet

Reactors

Low energy, but high fluxes possible

Next-generation neutrino beams

Low-energy tail of the neutrino spectrum of LBNF

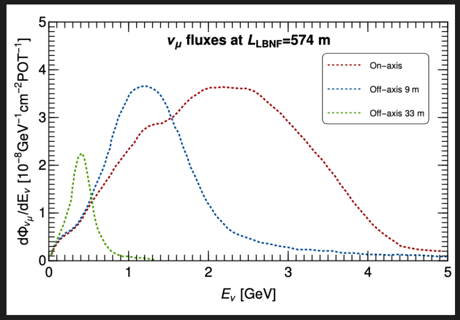

Aristizabal+ PRD 104, 033004 (2021)

Adapted from K. Scholberg @ CNNP2017 and Snowmass 2021 2203.07361

LOW-ENERGY NEUTRINOS FROM ARTIFICAL SOURCES

Radioactive source ^{51}Cr

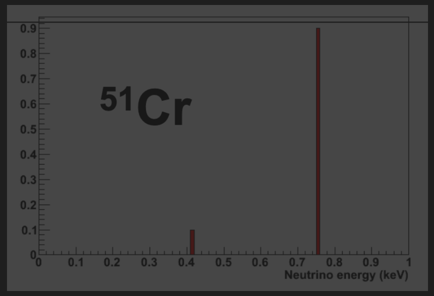

Electron-capture decaying isotope
4 monochromatic lines
very short baseline
low energy challenging

Stopped pions (Decay at rest)

High energy, pulsed beam

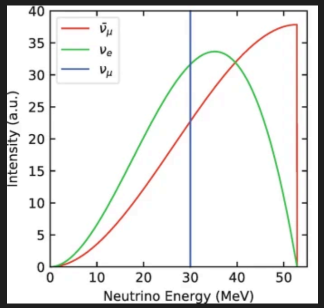

Scolz, https://doi.org/10.1007/978-3-319-99747-6_3

Reactors

Low energy, but high fluxes possible

Credit: neutrinos.fnal.gov

Beam induced radioactive sources (IsoDAR)

Higher energy than reactors
Does not exist yet

Next-generation neutrino beams

Low-energy tail of the neutrino spectrum of LBNF

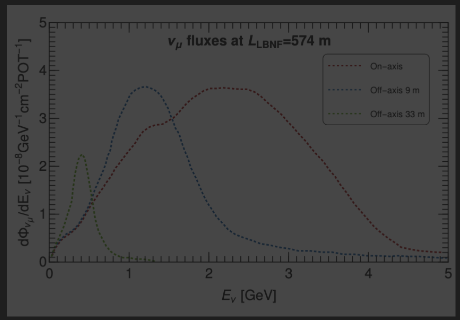

Aristizabal+ PRD 104, 033004 (2021)

Adapted from K. Scholberg @ CNNP2017 and Snowmass 2021 2203.07361

STOPPED-PION (π-DAR) NEUTRINOS

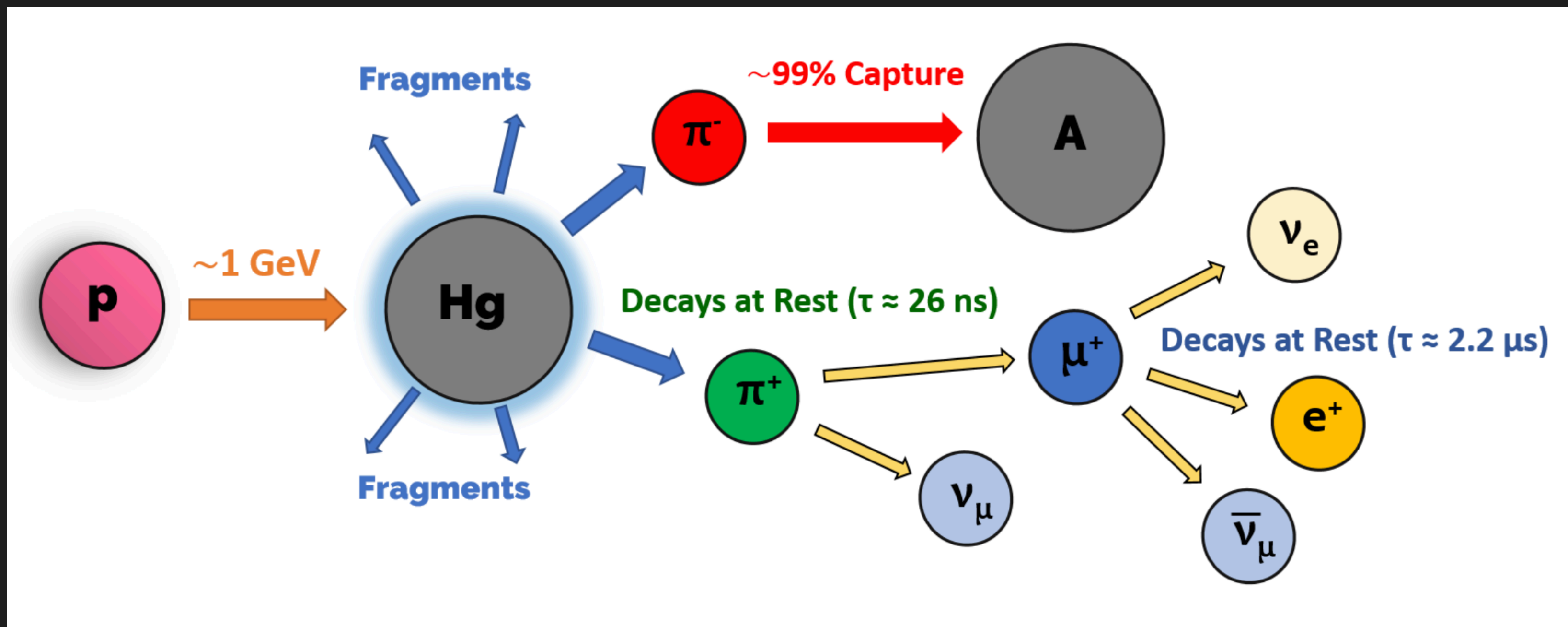

Credit: M. Green @ Magnificent CEvNS 2019

$$\pi^+ \rightarrow \mu^+ + \nu_\mu$$

Prompt monochromatic ν_μ from stopped pion decays

$$\mu^+ \rightarrow e^+ + \bar{\nu}_\mu + \nu_e$$

Delayed

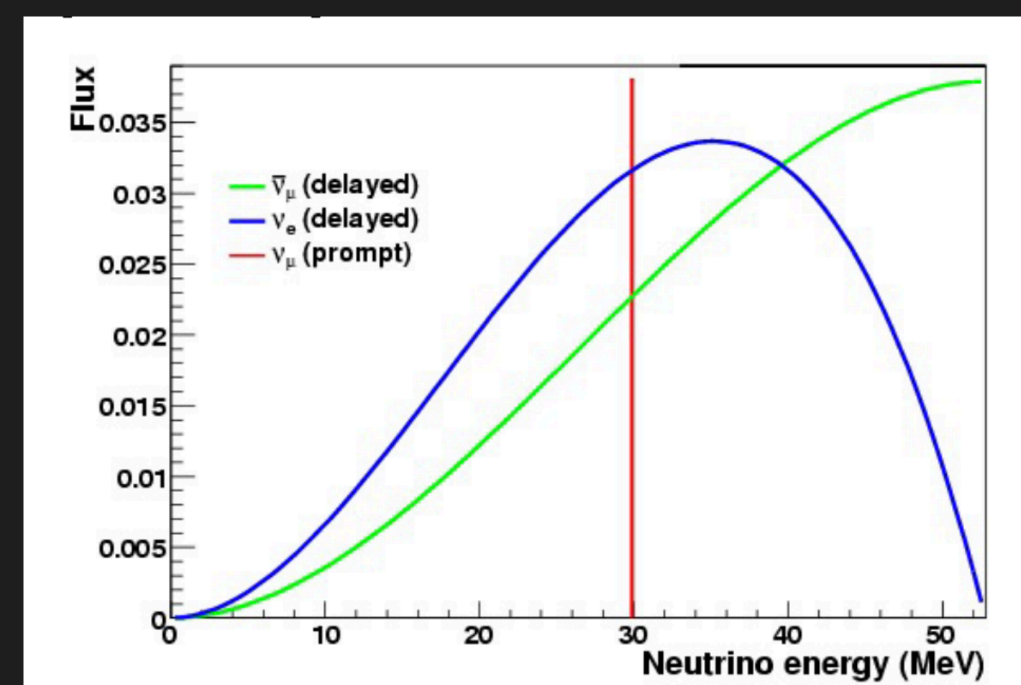

D. Akimov et al. (COHERENT). 2110.07730

STOPPED-PION (π-DAR) NEUTRINOS

- Spallation Neutron Source (SNS) at Oak Ridge National Laboratory (USA).
- Lujan center at Los Alamos Neutron Science Center LANSCE (USA).
- China Spallation Neutron Source CSNS (China).
- European Spallation Source (ESS) under construction (Sweden)

- High energy
- Pulsed beam → good background rejection
- Neutron backgrounds

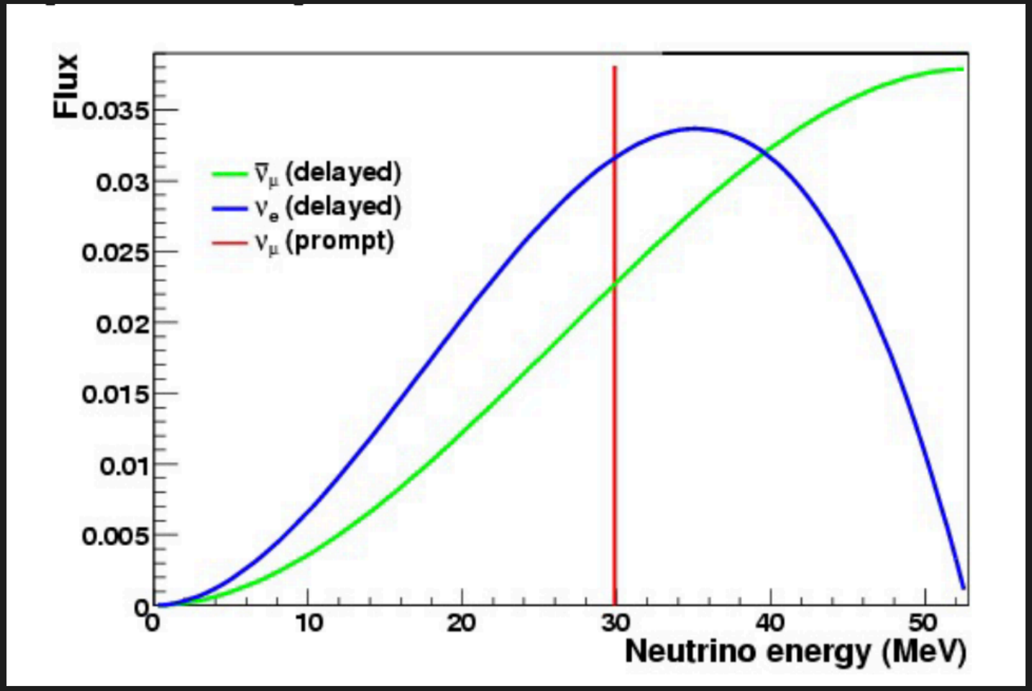

D. Akimov et al. (COHERENT). 2110.07730

TIME DISTRIBUTION OF A π-DAR NEUTRINO SOURCE (SNS)

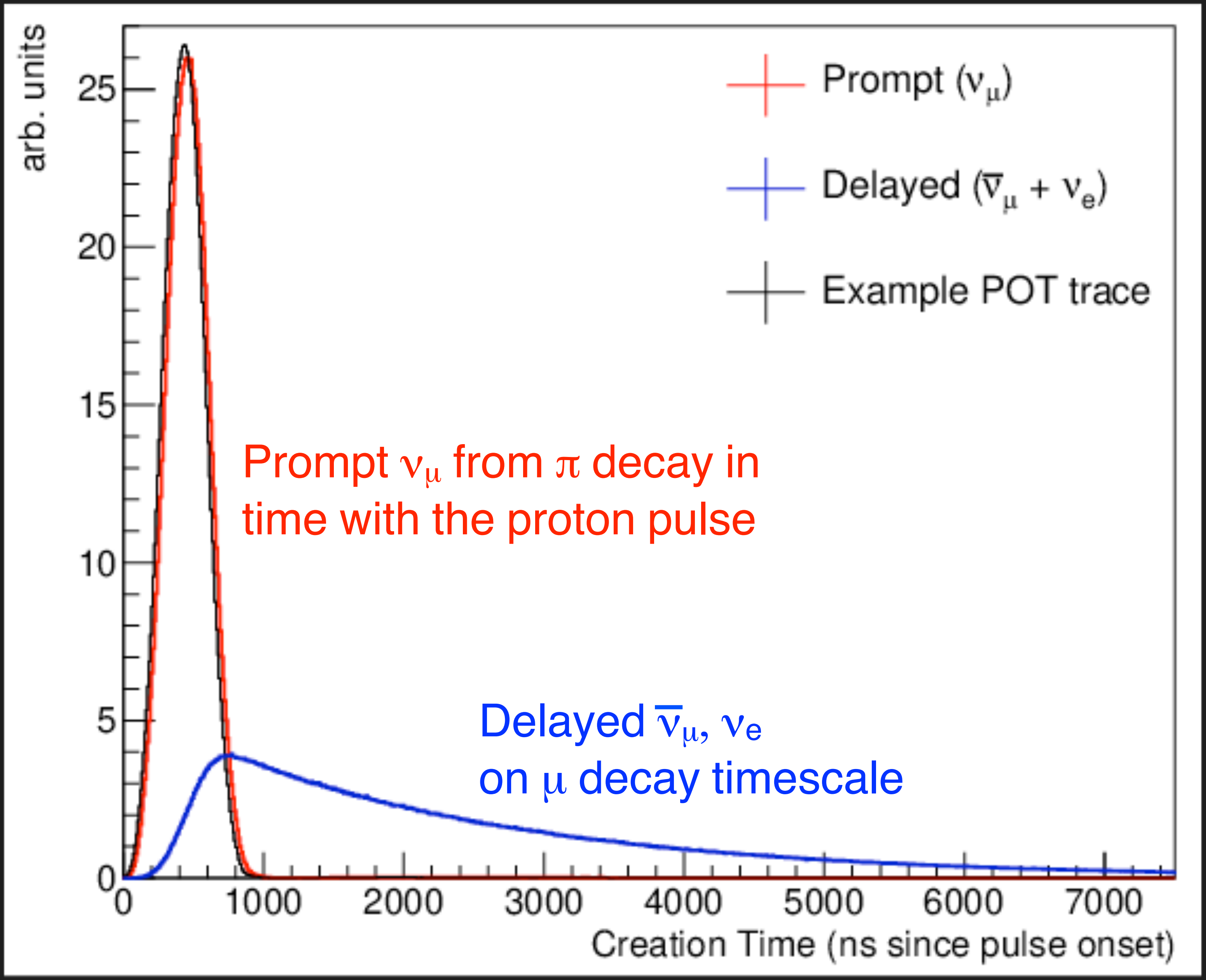

Snowmass 2021 2203.07361

NEUTRINOS FROM NUCLEAR REACTORS

PROs:
- Copious sources of electron antineutrinos
- Low energy (≲ 10 MeV): coherence condition for the recoil is largely preserved

CONs:
- Even smaller recoil energies
- Large backgrounds (although reactor-off allows to measure bckg)
- Only one flavor accessible

Credit: constellationenergy.com

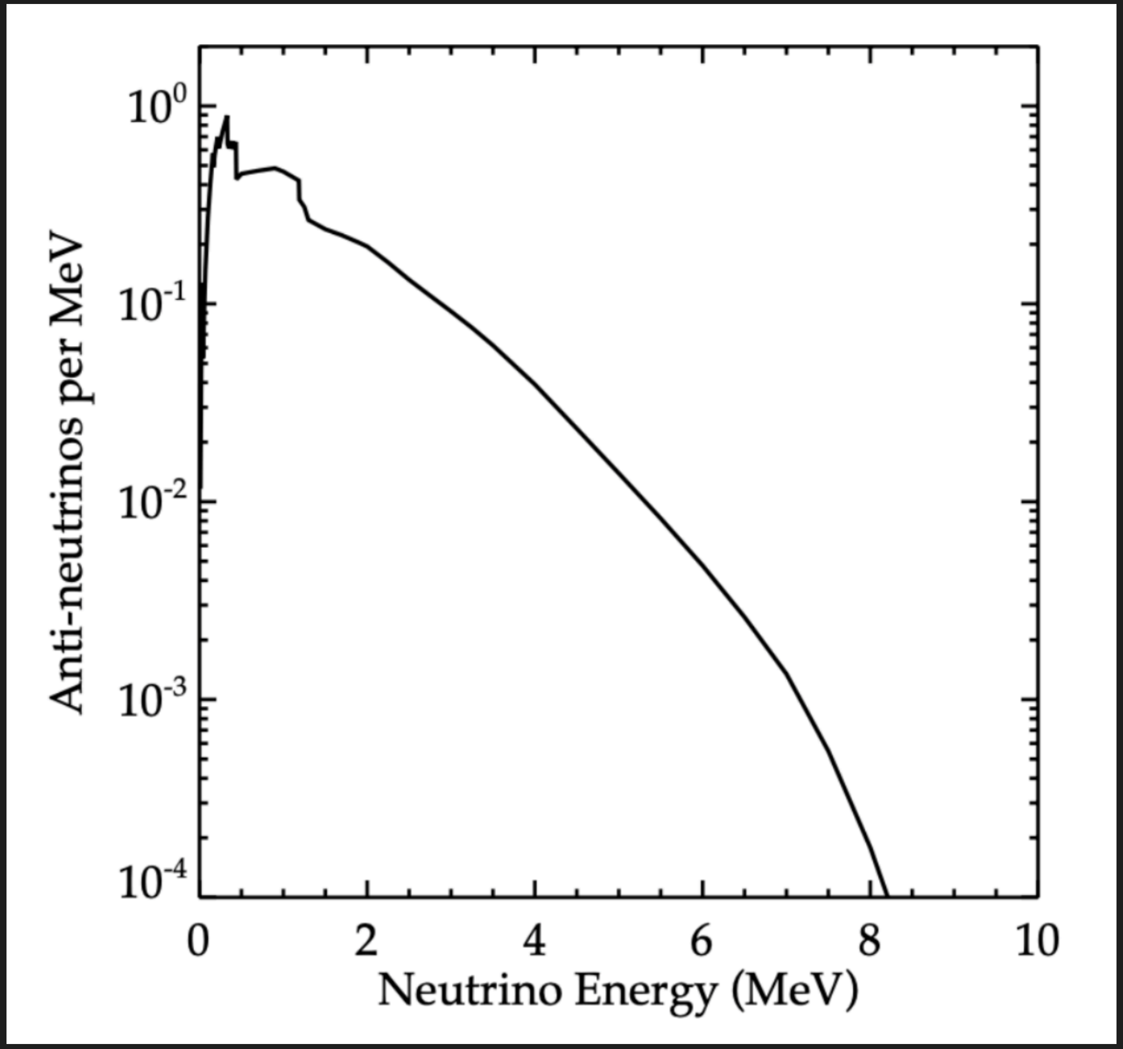

Snowmass 2021 2203.07361

EXPERIMENTS AND DETECTION

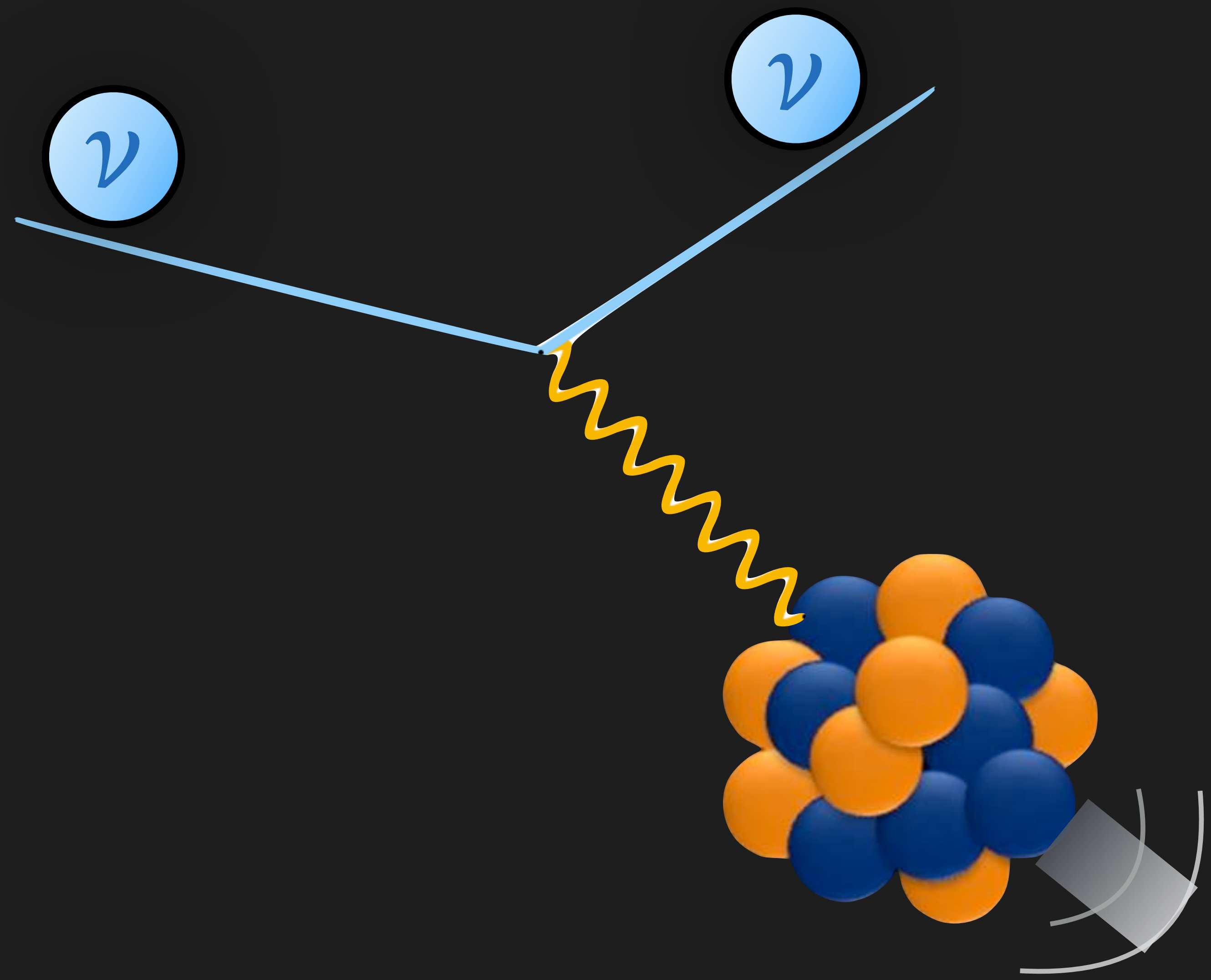

LOW-ENERGY NUCLEAR RECOIL DETECTION STRATEGIES

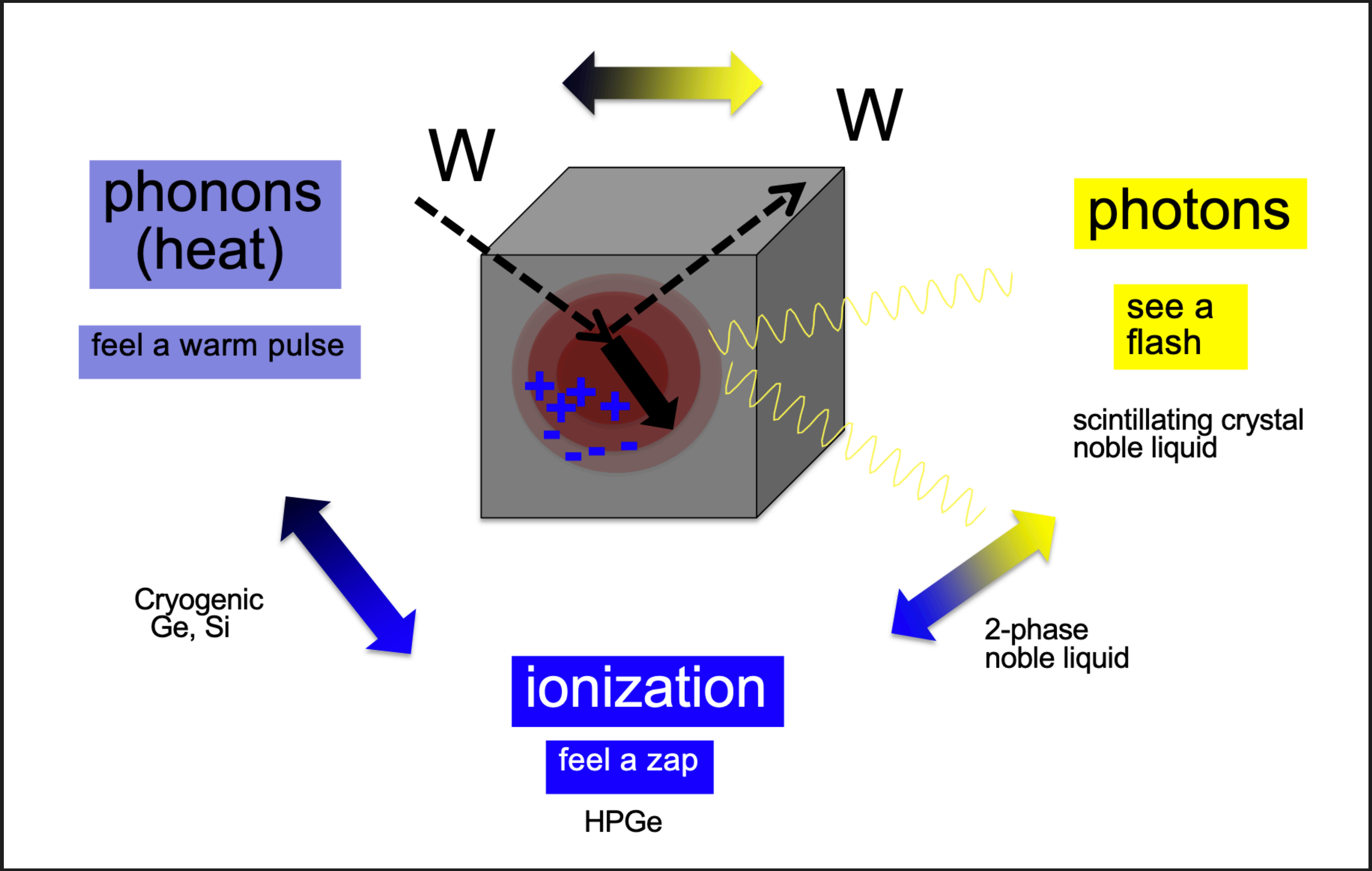

Credit to K. Scholberg @INSS 2021 and
http://dmrc.snu.ac.kr/english/intro/intro1.html

CEvNS EXPERIMENTS WORLDWIDE

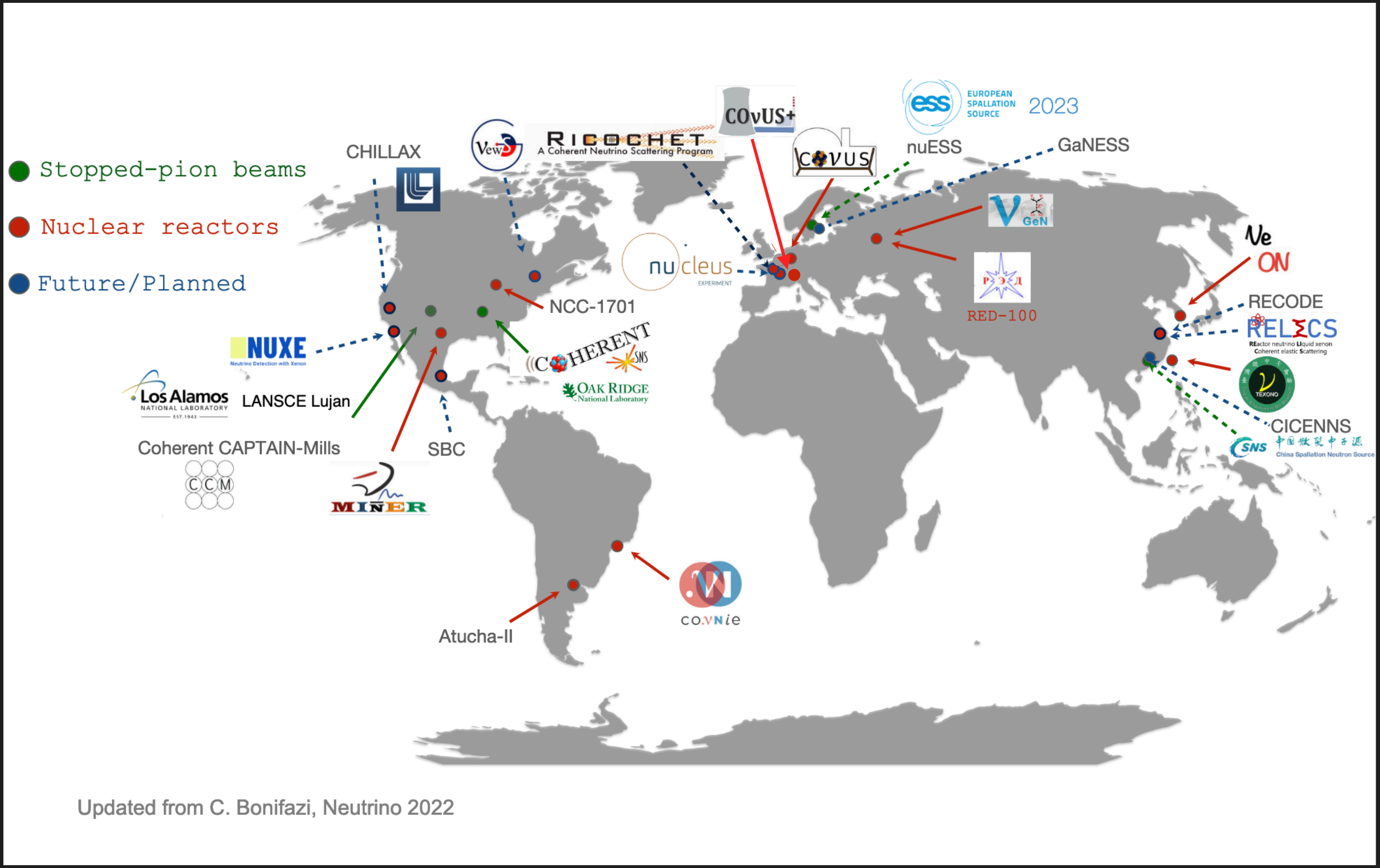

Credit to I. Nasteva @NEUTRINO 2024

(INCOMPLETE! LIST OF) CEνNS EXPERIMENTS

Experiment	T_{th}	Baseline (m)	Target	Mass (kg)	Technology	Source	Neutrino flux ($\nu/cm^2/s$)
COHERENT	6.5 $\mathrm{keV_{nr}}$	19.3	CsI[Na]	14.57	Scintillating crystal	π-DAR SNS	4.3×10^7
	1.5 $\mathrm{keV_{ee}}$	22	Ge	10.66	HPGe PPC		
	20 $\mathrm{keV_{nr}}$	29	LAr	2×10^3	Single phase		
	13 $\mathrm{keV_{nr}}$	28	NaI[Tl]	185*/3388	Scintillating crystal		
CCM	10-20 keV	20-40	LAr	10^4	Scintillation	π-DAR Lujan	
ESS*			CsI, Ge, Xe, Ar			π-DAR	
CICENNS*	2 $\mathrm{keV_{nr}}$	10.5	CsI(Na)	300	Scintillation	π-DAR	2×10^7
NCC-1701 (DRESDEN-II)	200 $\mathrm{eV_{ee}}$	8	Ge	3	HPGe	NPP 2.9 GW	8.1×10^{13}
CONUS	210 $\mathrm{eV_{ee}}$	17	Ge	4	HPGe	NPP 3.9 GW	2×10^{13}
CONUS+	150 $\mathrm{eV_{ee}}$	20.7	Ge	4	HPGe	NPP 3.6 GW	1.45×10^{13}
MINER	100 $\mathrm{eV_{nr}}$	1	$Ge/Si/Al_2O_3$	2-10	cryogenic	NPP 1 MW	1×10^{12}
CONNIE	15 $\mathrm{eV_{ee}}$	30	Si	0.5×10^{-3}	Si CCDs	NPP 3.9 GW	7.8×10^{12}
Ricochet	300 $\mathrm{eV_{nr}}$	8.8	Ge,Zn,Al, Sn	0.68	cryogenic	NPP 58 MW	1.6×10^{12}
NUCLEUS	200 $\mathrm{eV_{ee}}$	77, 102	$CaWO_4$ Al_2O_3	10^{-2}	Cryogenic $CaWO_4$ Al_2O_3 calorimeter array	NPP 8.54 GW	1.7×10^{12}
RED100	500 eV	19	Xe	200	LXe dual phase	NPP 3.1 GW	1.35×10^{13}
vGEN	200 $\mathrm{eV_{ee}}$	11-12	Ge	1.4	HPGe	NPP 3.1 GW	5.4×10^{13}
TEXONO	200 $\mathrm{eV_{ee}}$	28	Ge	1.43	p-PCGe	NPP 2 × 2.9 GW	6.4×10^{12}
NEON	200 $\mathrm{eV_{ee}}$	23.7	Na(Tl)	16.7	scintillator	NPP 2 × 2.8 GW	$\sim \times 10^{13}$
SBC*	100 $\mathrm{eV_{ee}}$		Ar	10		NPP 2 × 2.9 GW	

WHICH EXPERIMENTS HAVE OBSERVED CEνNS?

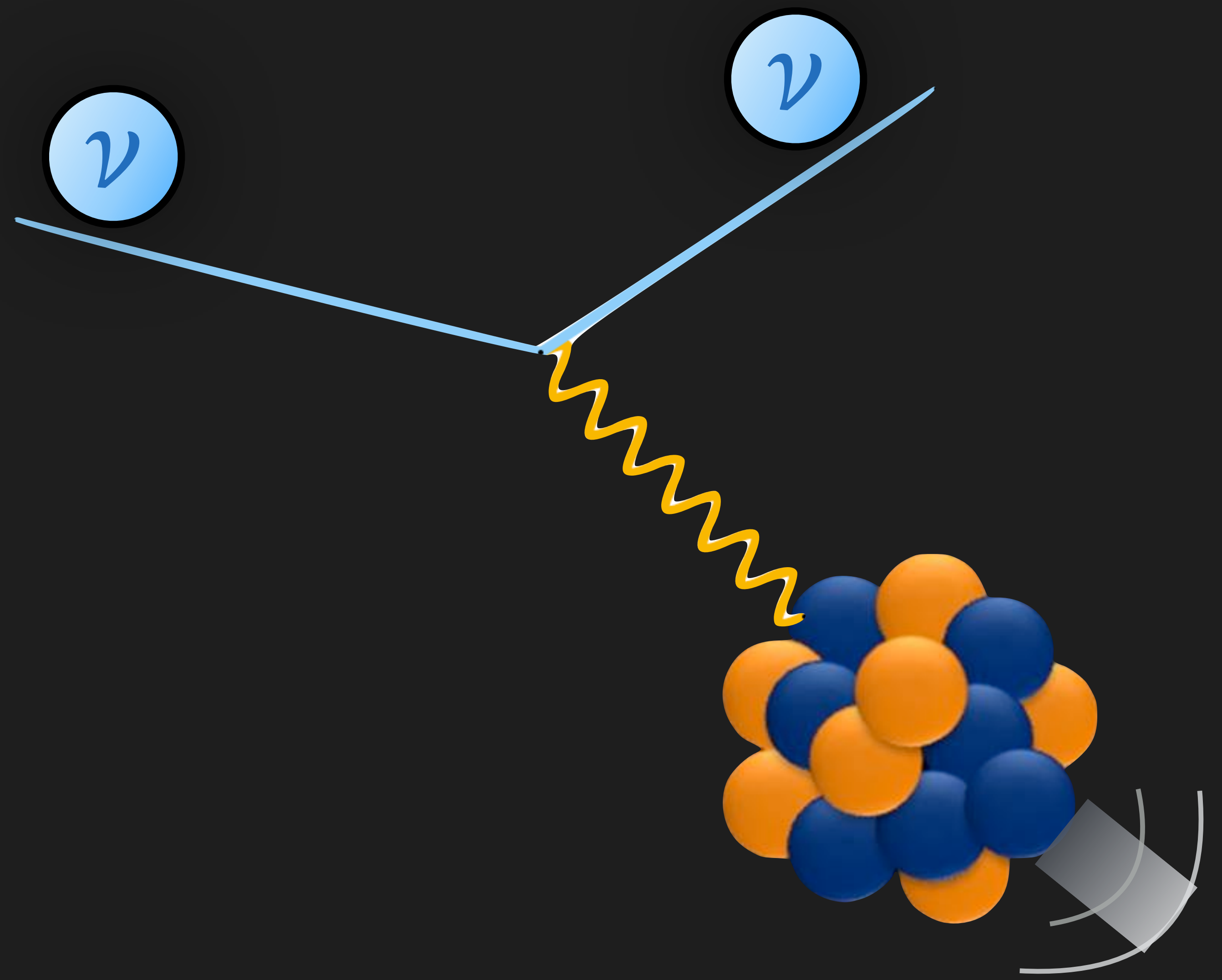

1st OBSERVATION OF CEvNS BY COHERENT

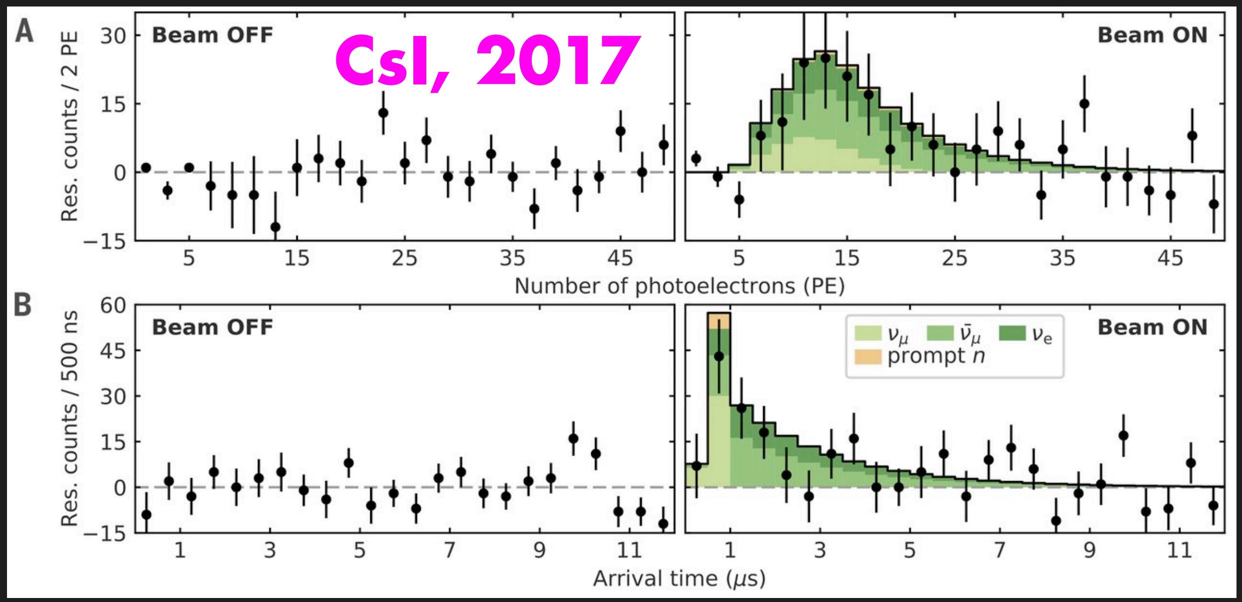

Observation at 6.7σ confidence level
~ 130 events observed

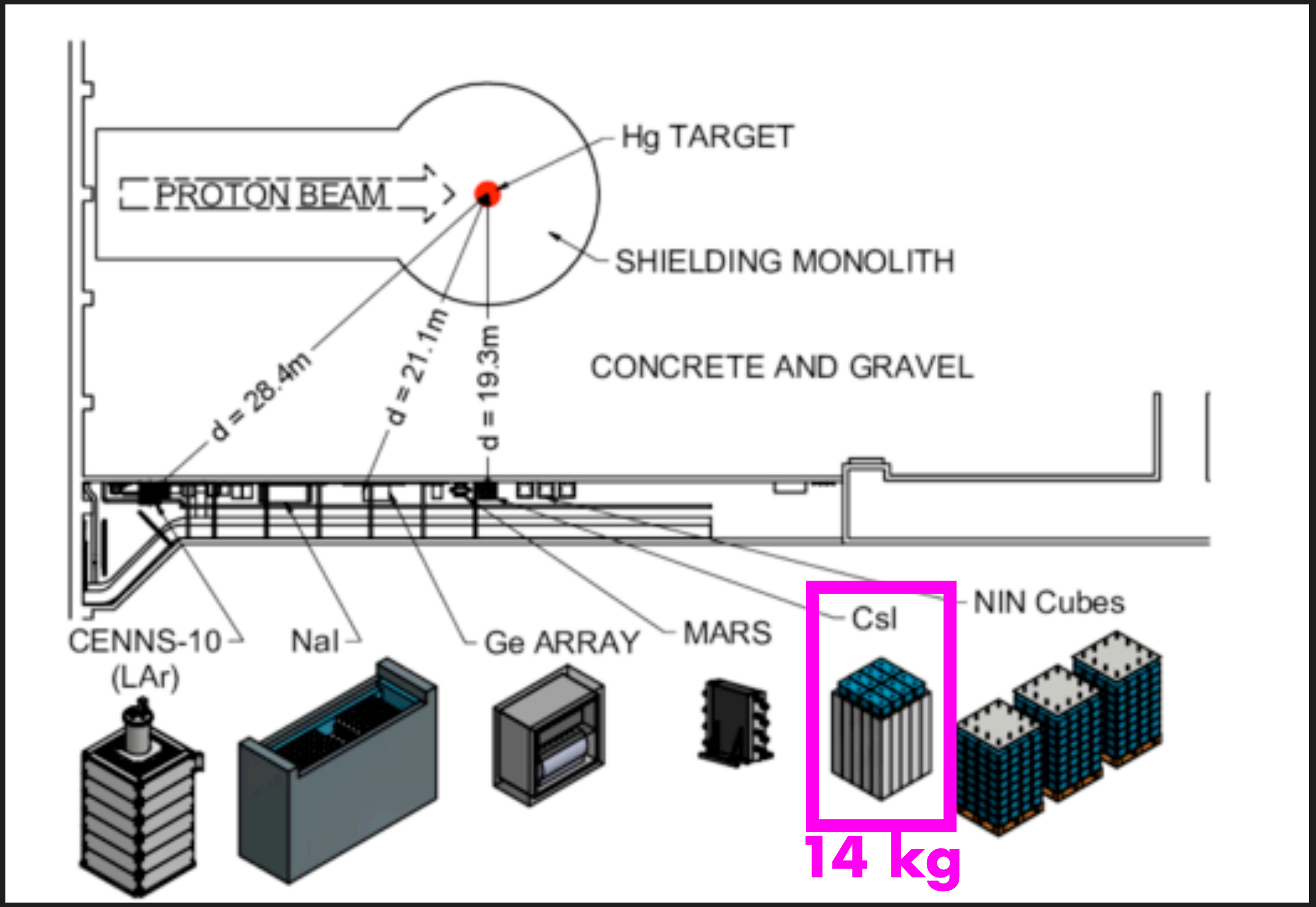

COHERENT-CsI[Na] was the world's smallest working neutrino detector!

D. Akimov et al. (COHERENT) Science 357, 1123–1126 (2017)

COHERENT CsI MEASUREMENT

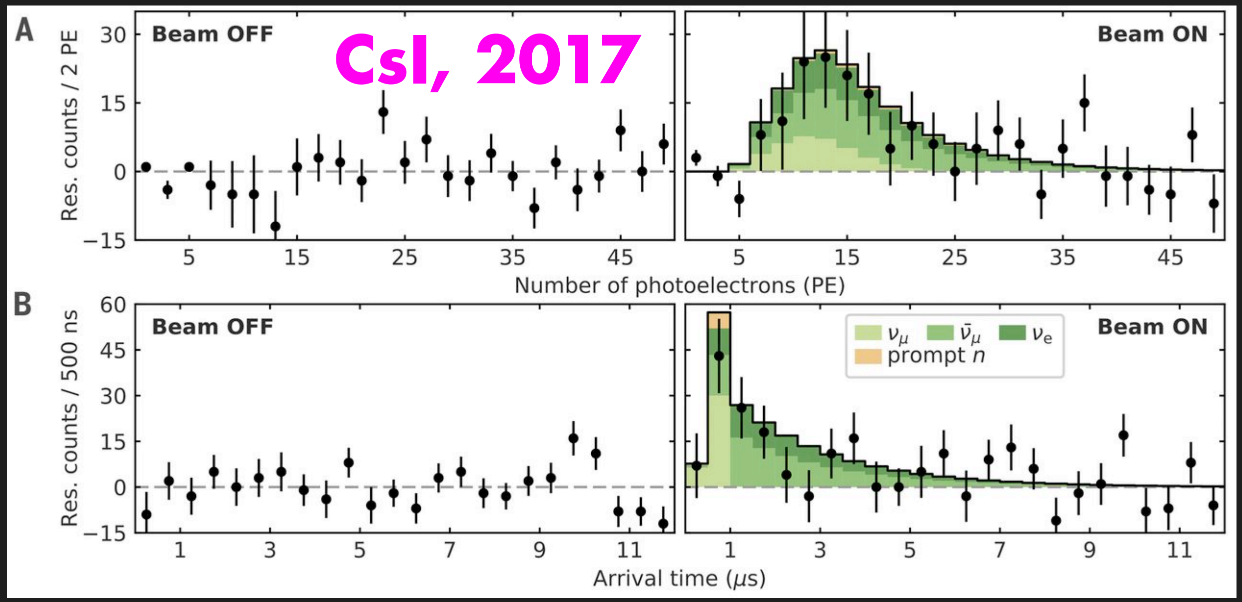

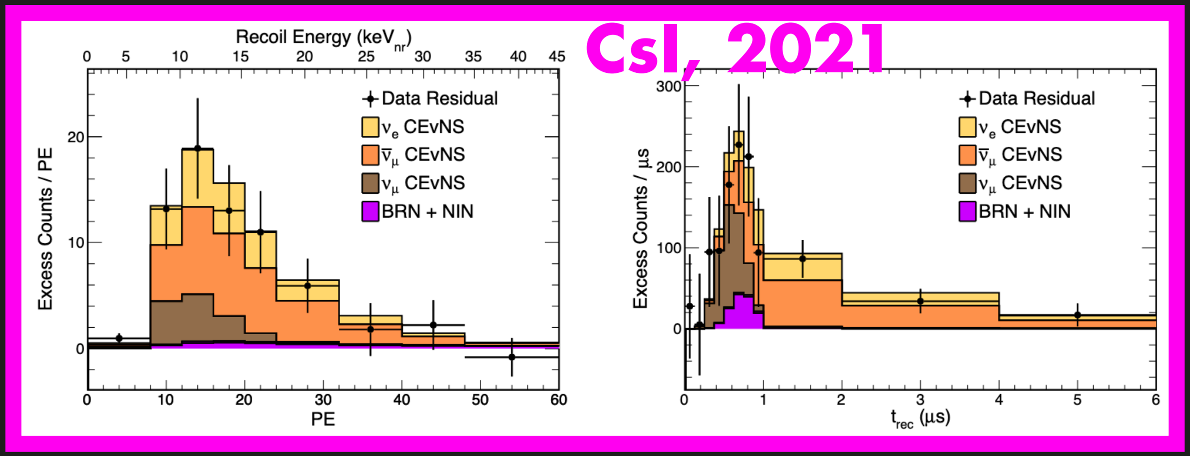

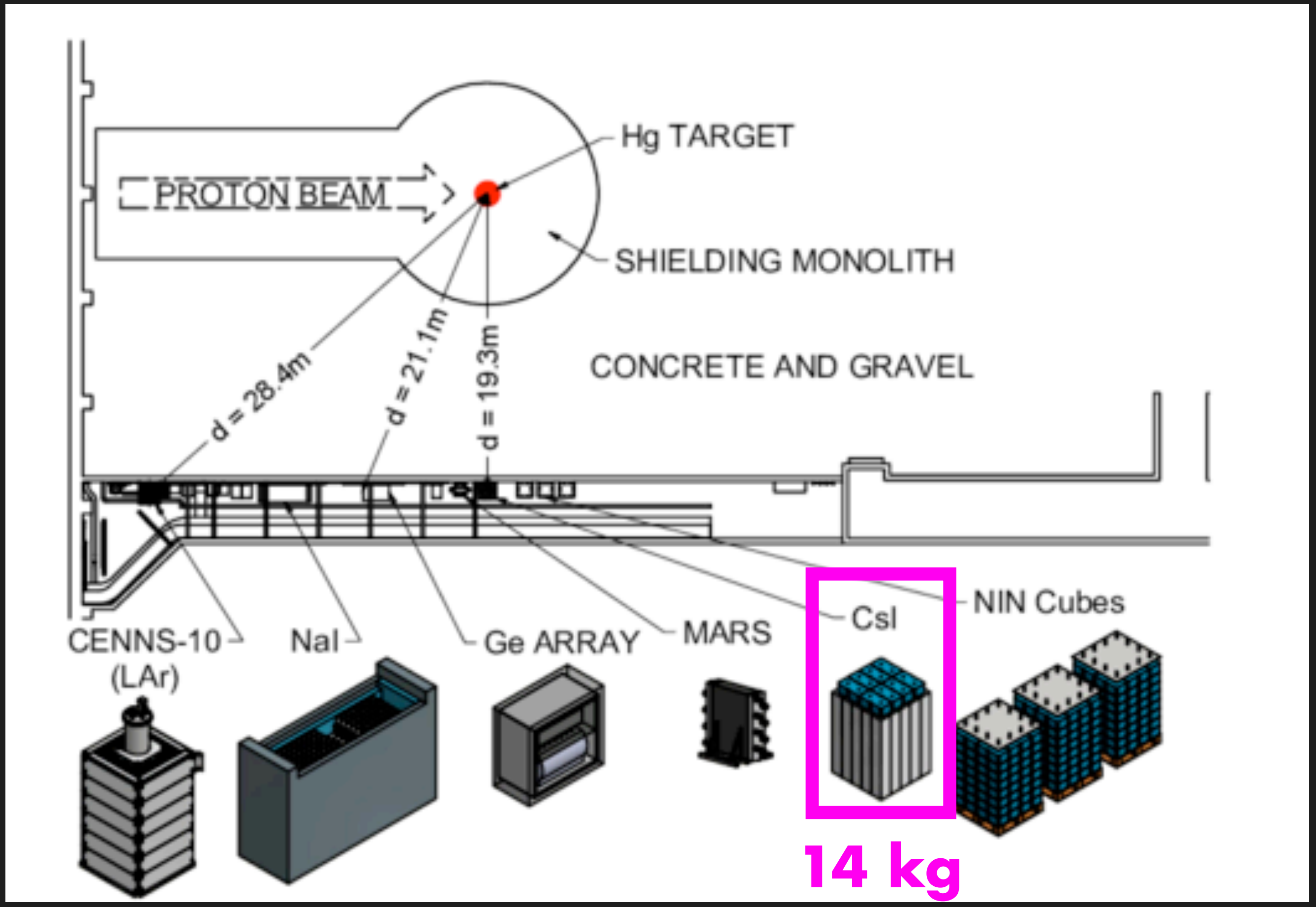

D. Akimov et al. (COHERENT) Science 357, 1123–1126 (2017)
D. Akimov et al. (COHERENT) Phys. Rev. Lett. 129, 081801

COHERENT CsI MEASUREMENT

Full CsI[Na] dataset 2.2 times bigger, before decommissioning in 2019.
Updated scintillator response model, improved systematic uncertainties

Reject the no-CEvNS hypothesis at 11.6 σ level
~300 events observed

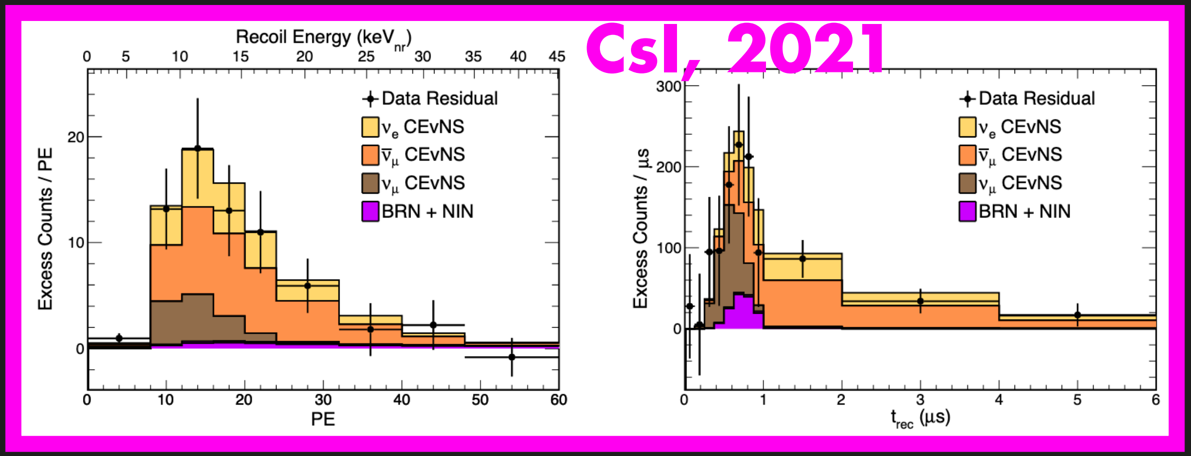

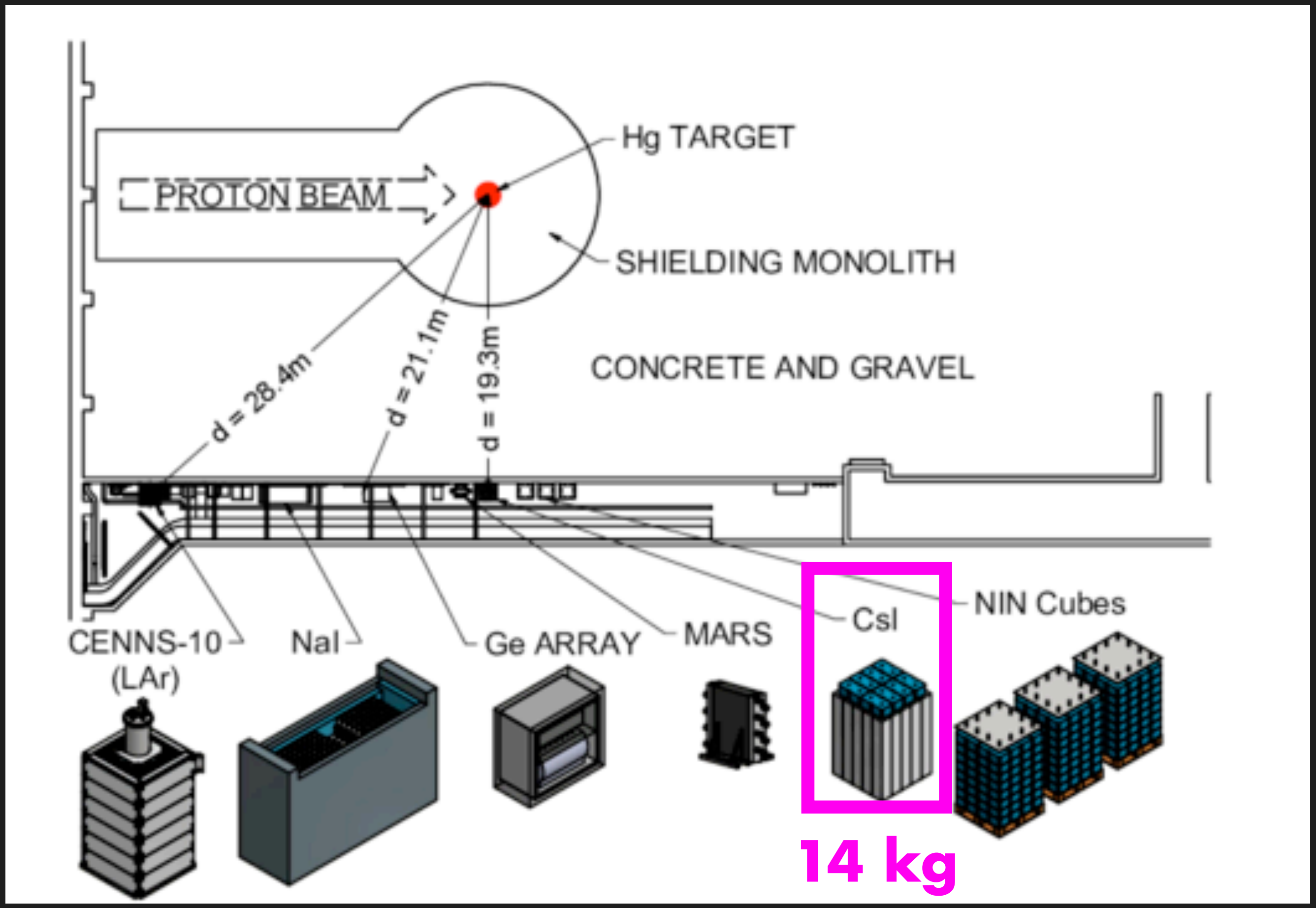

D. Akimov et al. (COHERENT) Science 357, 1123–1126 (2017)
D. Akimov et al. (COHERENT) Phys. Rev. Lett. 129, 081801

COHERENT LAr MEASUREMENT

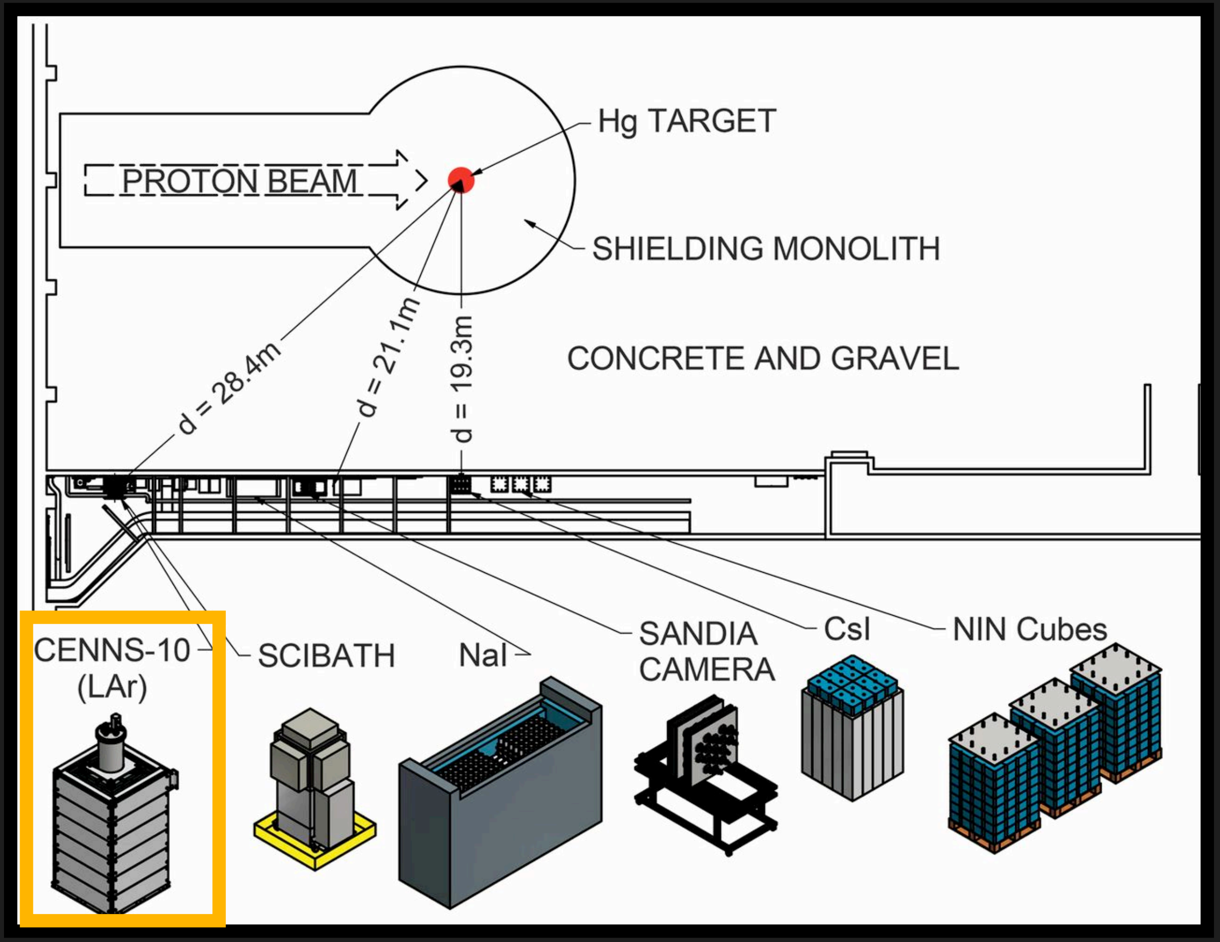

24 kg

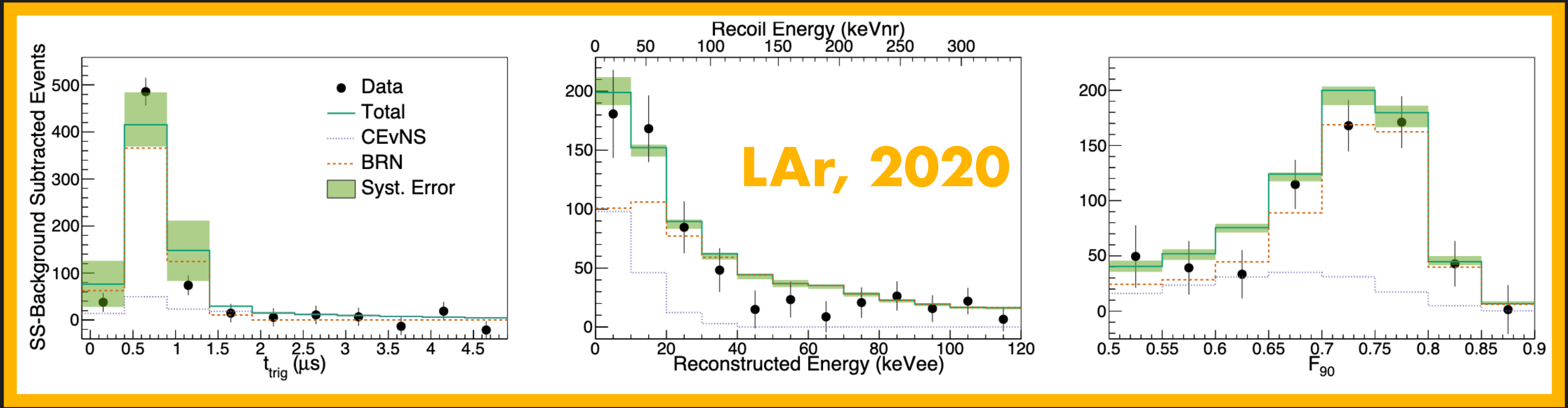

D. Akimov et al. (COHERENT). Phys. Rev. Lett. 126, 012002 (2021)

COHERENT LAr MEASUREMENT

CENNS-10 Lar single-case (scintillation) detector.
Reject the no-CEvNS hypothesis at 3.9 σ level
~150 events observed
First confirmation of its N^2 dependence

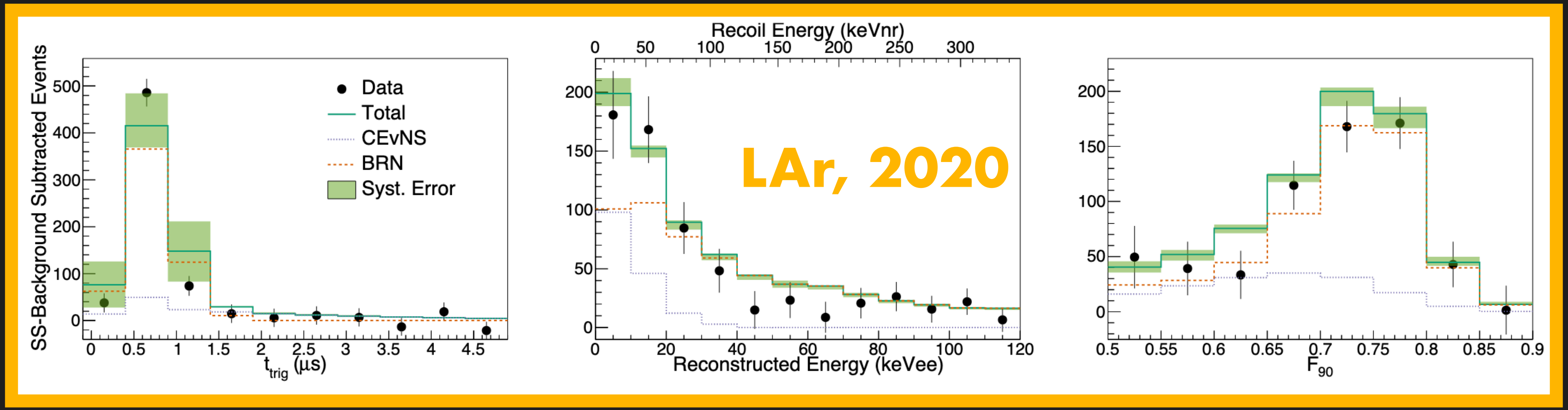

D. Akimov et al. (COHERENT). Phys. Rev. Lett. 126, 012002 (2021)

COHERENT-Ge MEASUREMENT

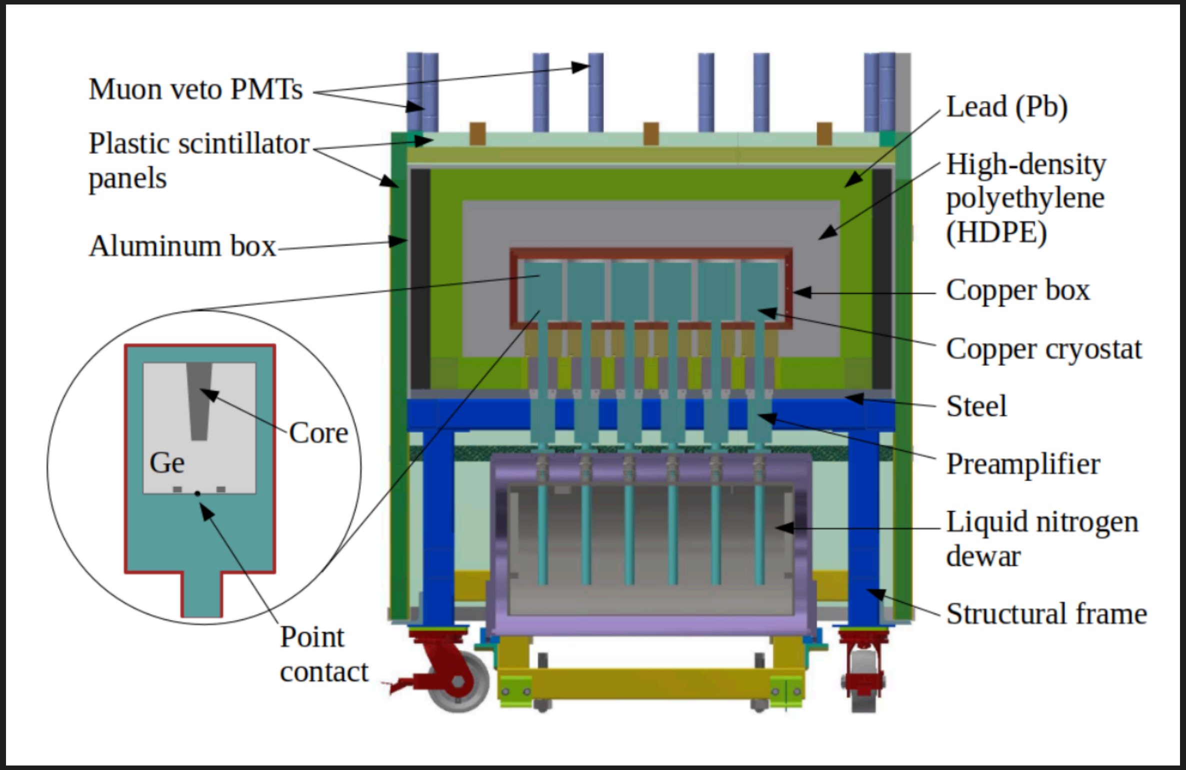

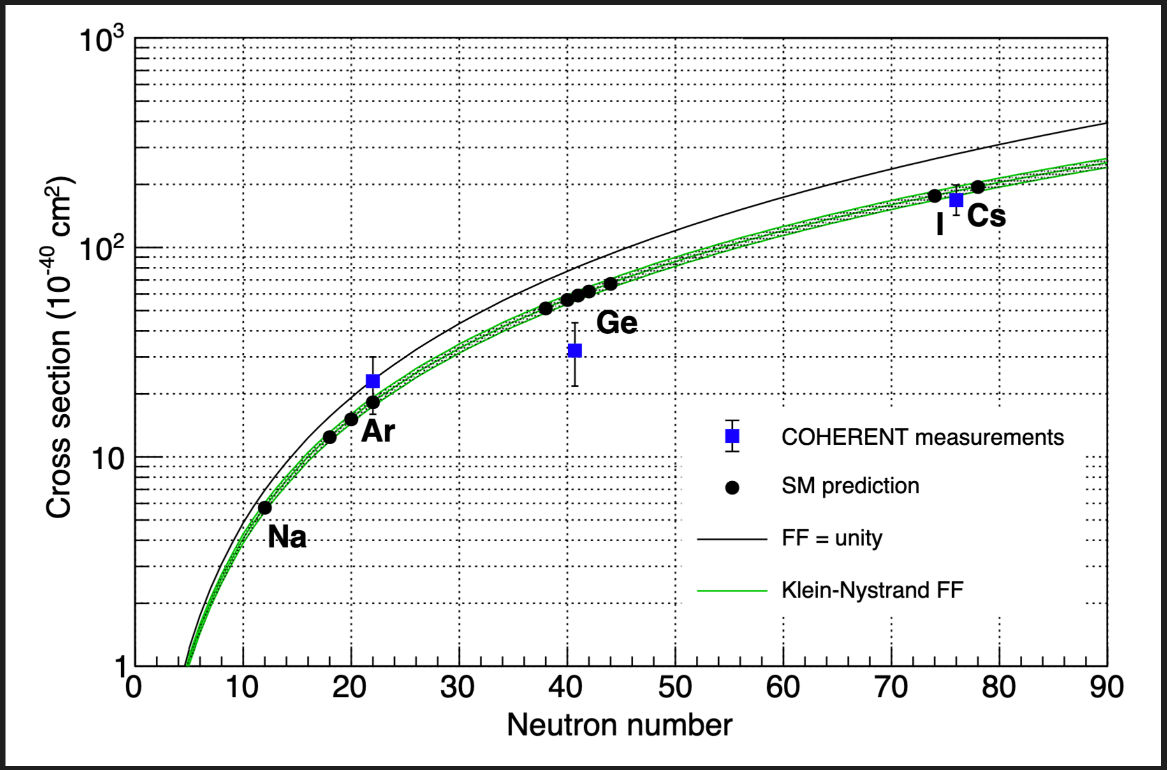

R. Bouabid @Magnificent CEvNS 2024

Ge-Mini detector system
~10 kg

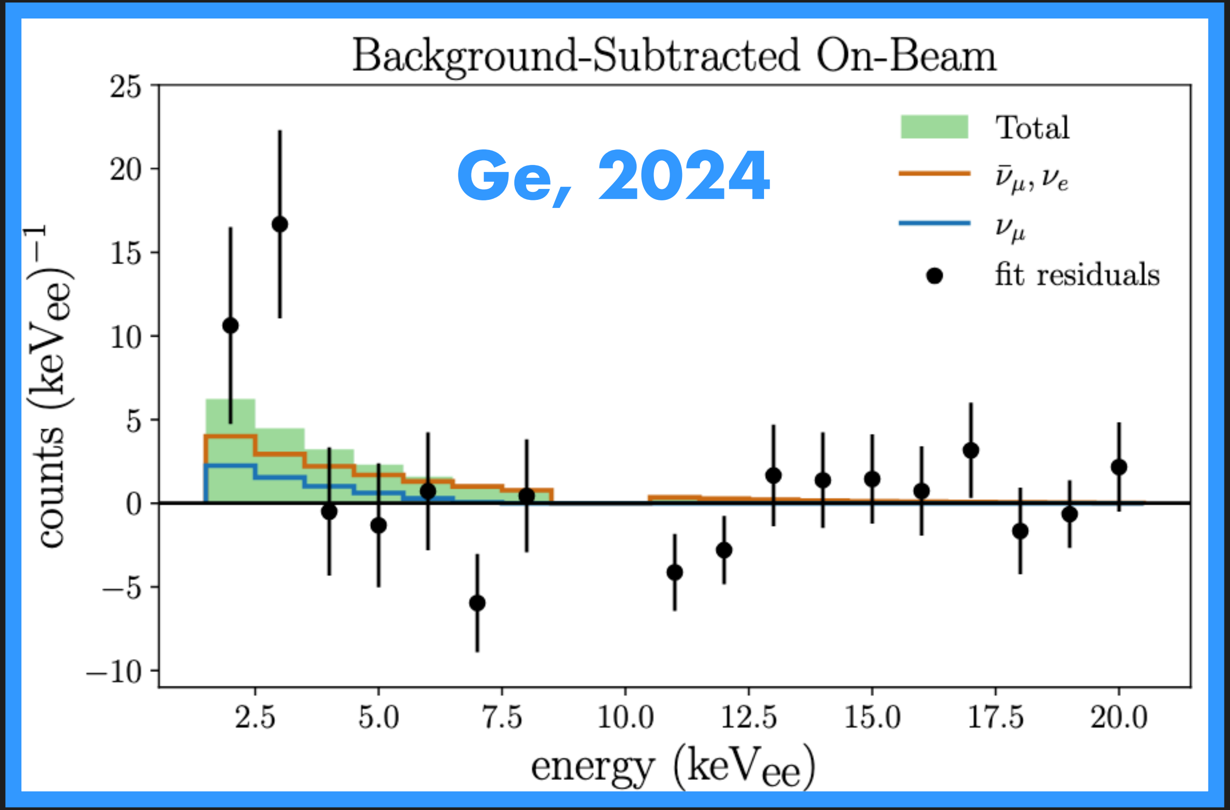

Reject the no-CEvNS hypothesis at 3.9 σ level
~20 events observed

S. Adamski et al. (COHERENT) arXiV: 2406.13806

EVIDENCE OF CEνNS ? AT NCC-1701 (DRESDEN-II REACTOR)

Neutrino source: Dresden-II boiling water reactor (USA) 2.96GW → 4.8 x10^{13} neutrinos/sec/cm^2

Detector: NCC-1701, a 2.924 kg ultra-low noise p-type point contact (PPC) Germanium detector

- low energy threshold (0.2 keV_{ee})
- distance to core: 10.39m
- 96.4-day exposure

CEνNS results: suggestive evidence of CEνNS is reported with strong preference (with respect to the background-only hypothesis)

- strongly dependent on quenching factor model

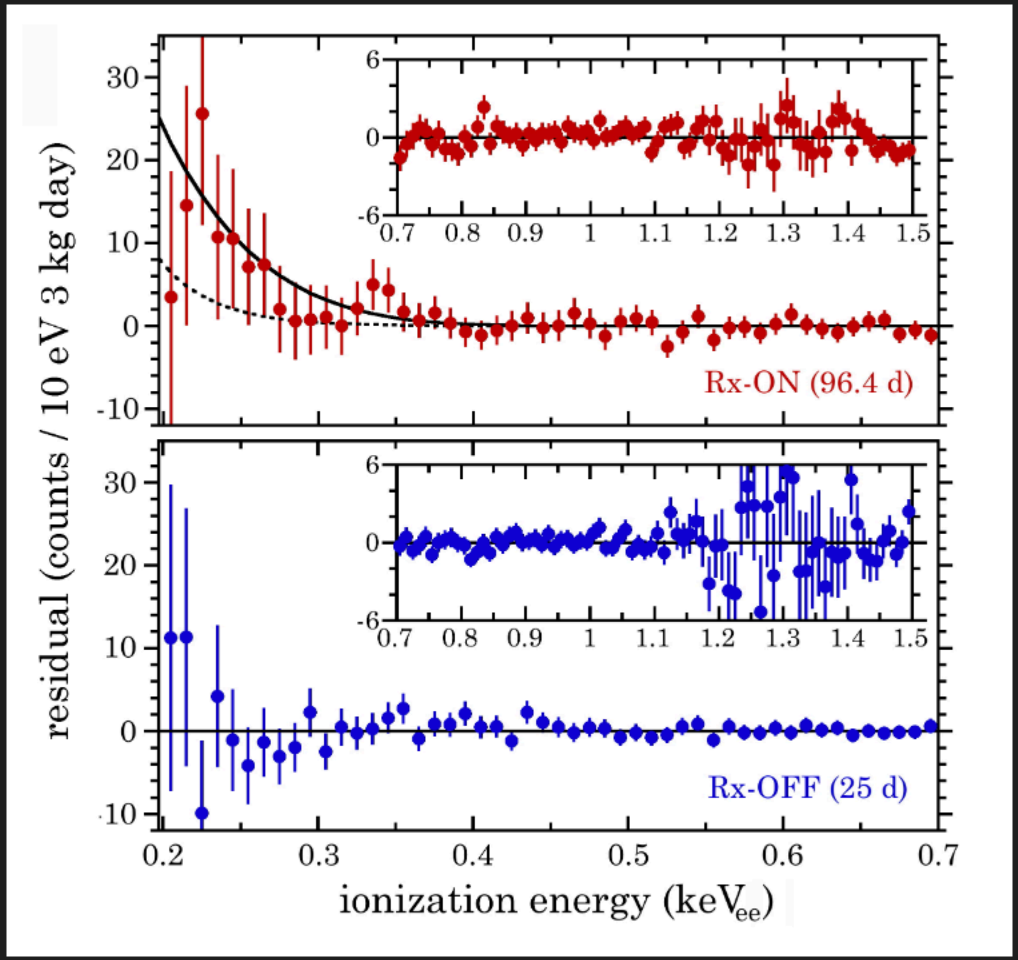

Colaresi, Collar et al. Phys. Rev. Lett. 129 (2022) 211802

EVIDENCE OF CEνNS ? AT NCC-1701 (DRESDEN-II REACTOR)

The quenching factor (QF) describes the observed reduction in ionization yield produced by a nuclear recoil when compared to an electron recoil of same energy

- often not (yet) well known at low recoil energies for CEνNS
- major uncertainty!

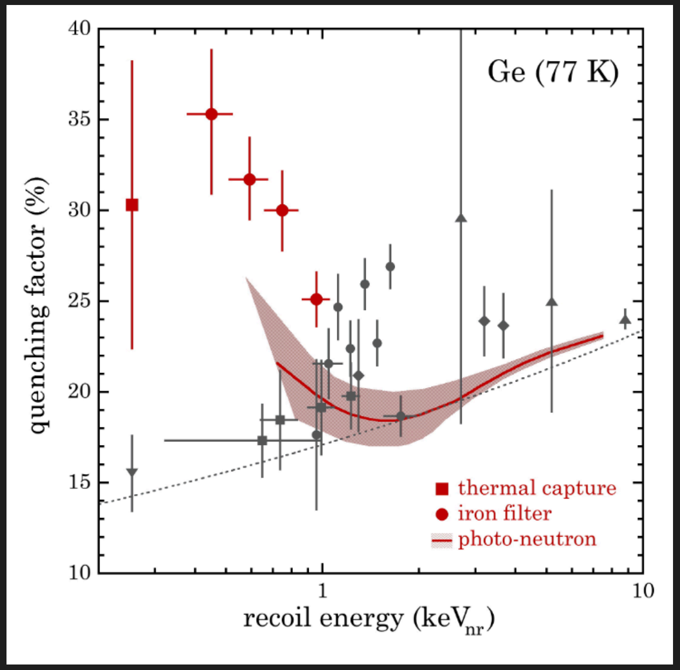

J.I. Collar et al, Phys. Rev. D 103, 122003

$$QF = E_{meas}/E_{nuclear\ recoil}$$

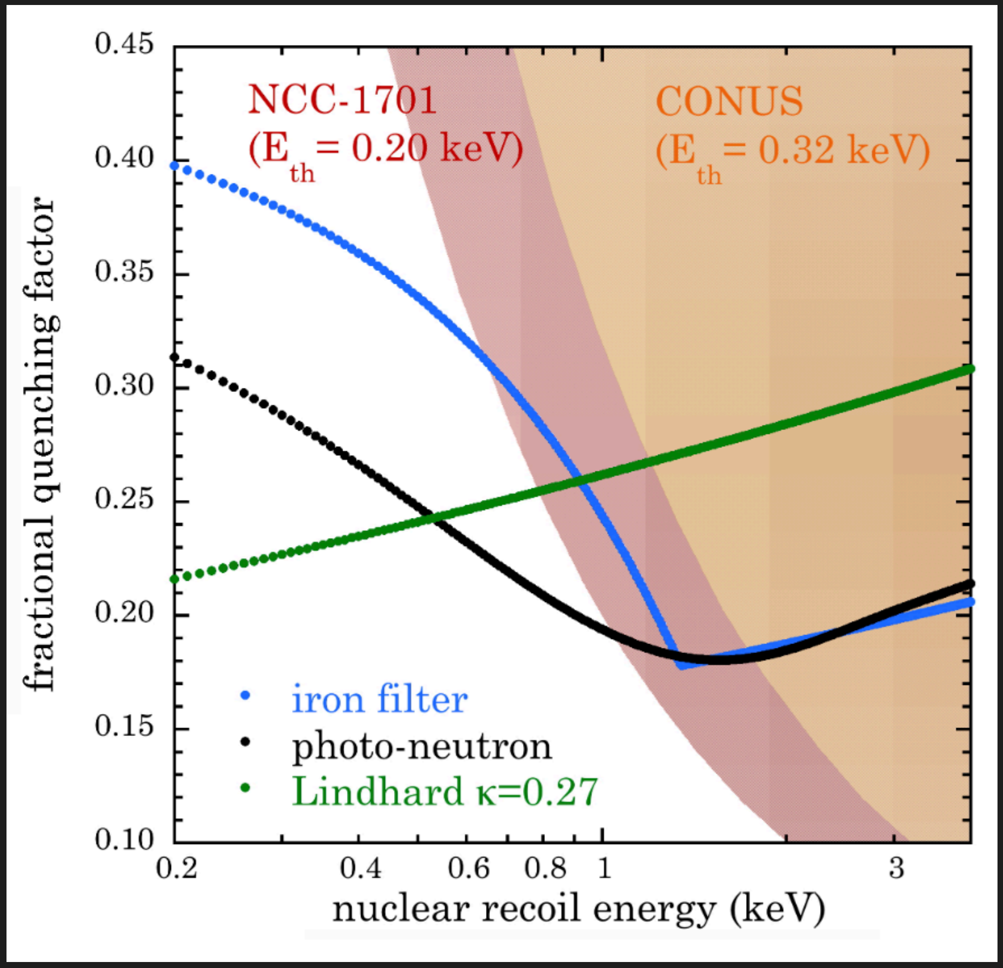

Colaresi et al., Phys. Rev. D 104, 072003 (2021)
Colaresi et al., 2202.09672 [hep-ex]

CONUS: Direct measurement of ionization quenching factor: k=0.162+-0.004 (compatible with Lindhard)

CONUS Phys. Rev. Lett. 126, 041804

XENONnT

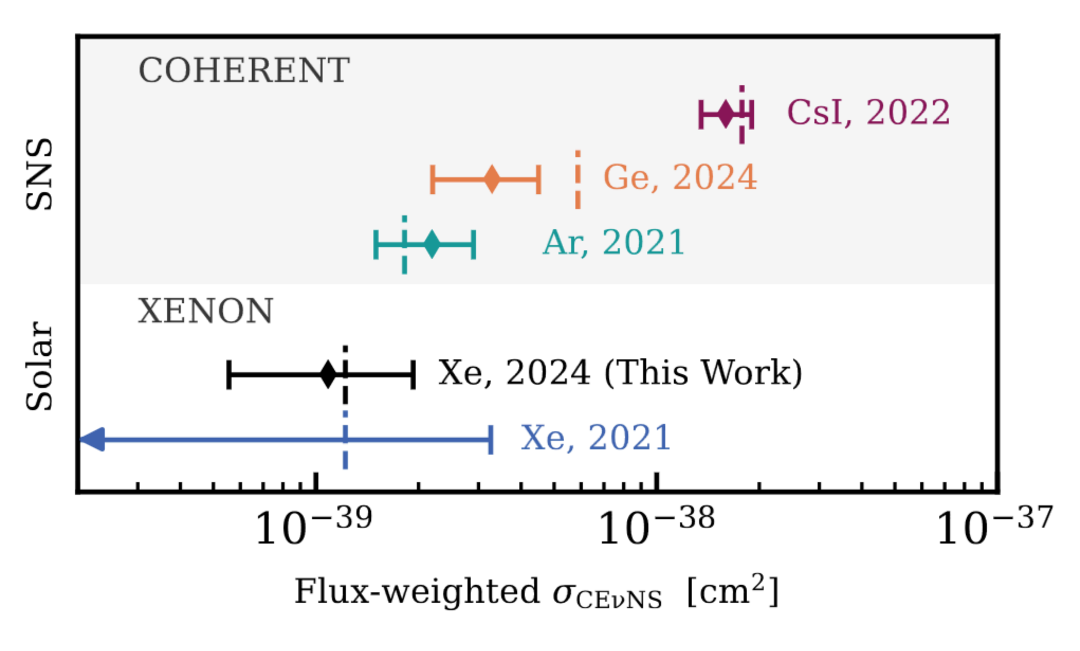

Aprile et al. arXiv:2408.02877v1

XENONnT "measures" the CEvNS signal in Xe from solar 8B neutrinos for the first time.

The background-only hypothesis is disfavored at 2.73σ

From Fei Gao's talk @ IDM 2024

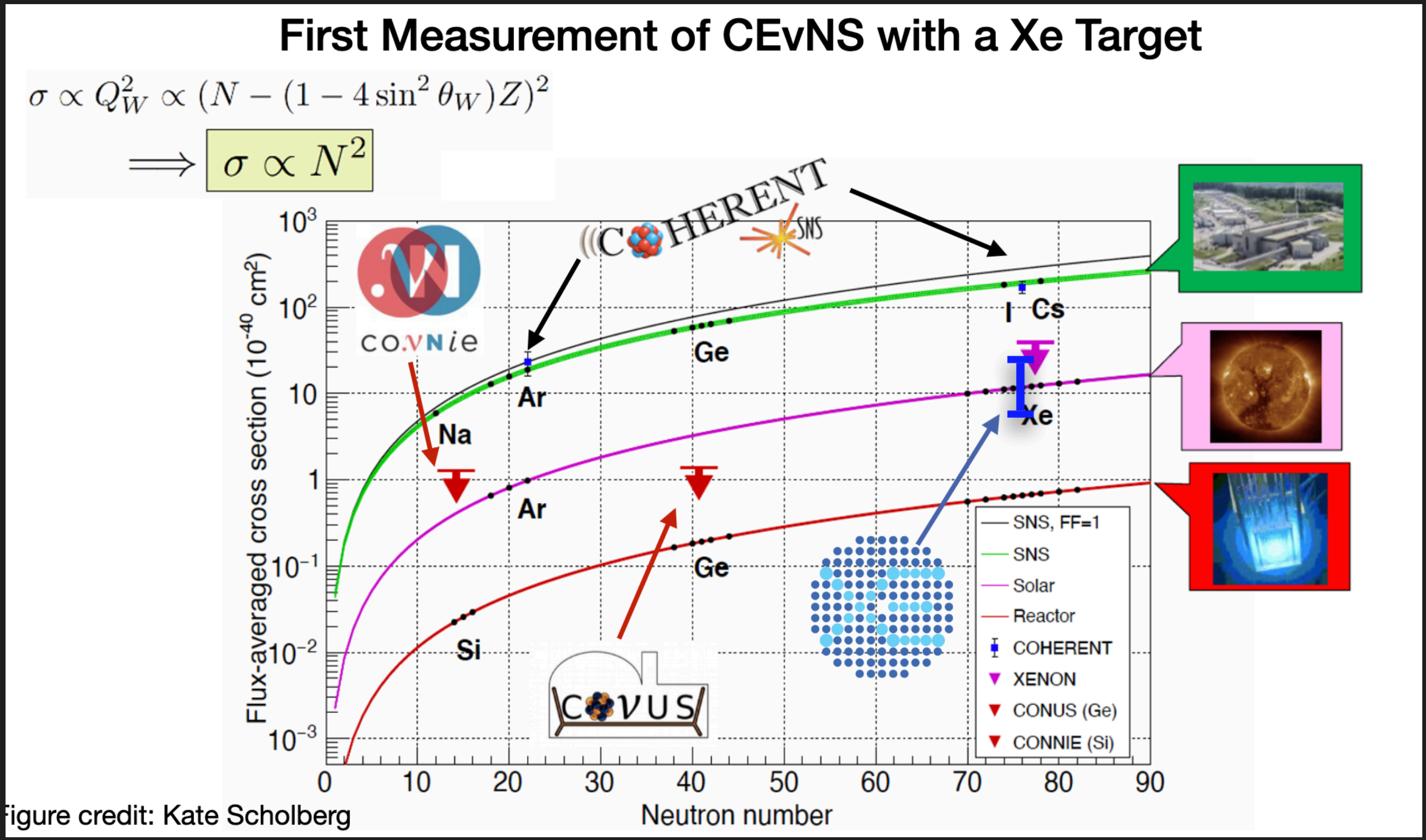

PandaX-4T

A combined analysis yields a best-fit ^{8}B neutrino signal of 3.5 (75) events from the scintillation and ionization (ionization-only) data sample.

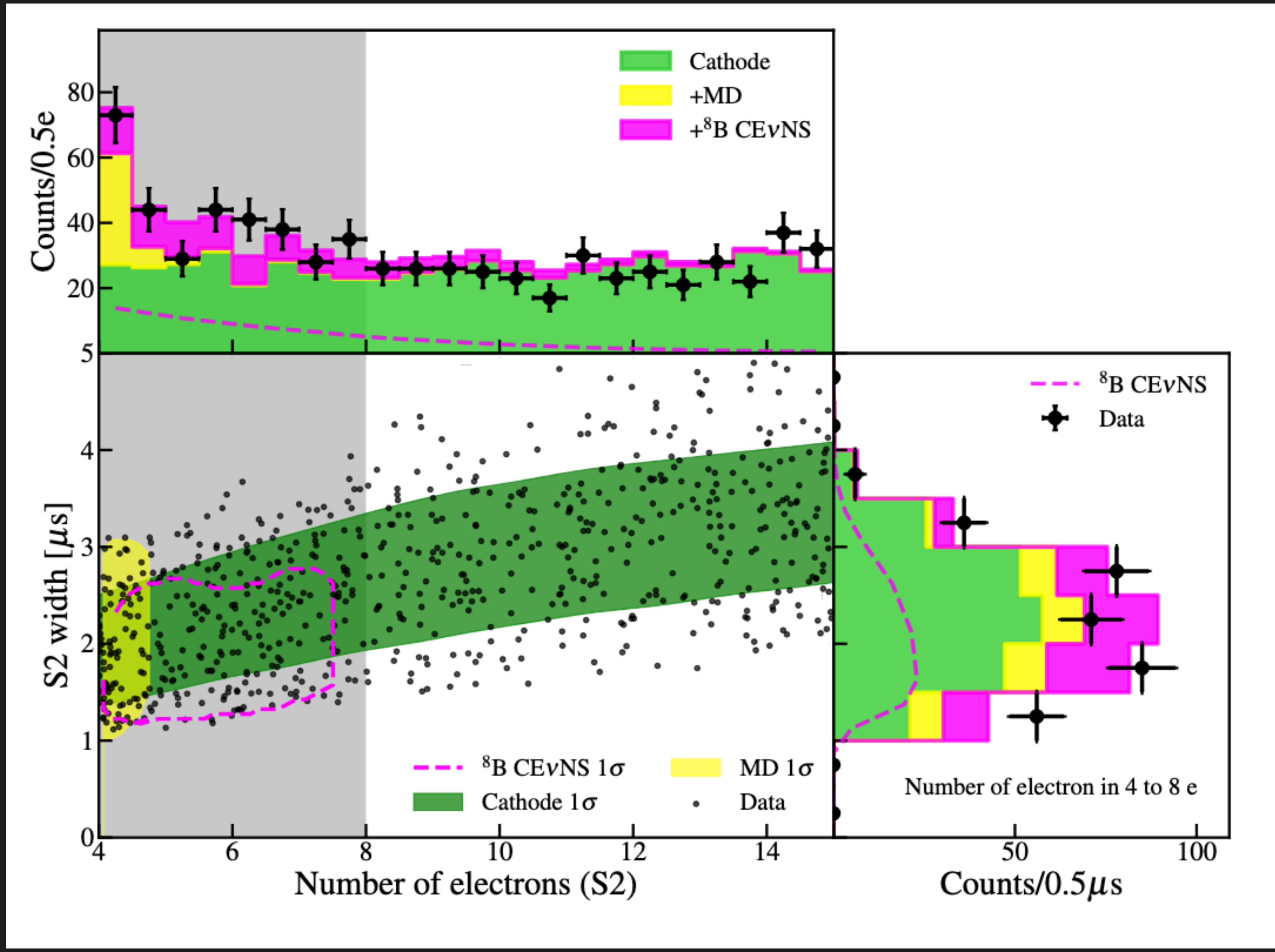

Z. Bo et al. (PandaX collaboration) arXiv:2407.10892

The background-only hypothesis is disfavored at 2.64 σ significance

LIST OF EXPERIMENTAL PAPERS

1. Coherent Elastic Neutrino-Nucleus Scattering Search in the νGeN Experiment, Phys.Part.Nucl.Lett. 21 (2024) 4, 680-682
2. First Measurement of SolarB Neutrino Flux through Coherent Elastic Neutrino-Nucleus Scattering in PandaX-4T, Zihao Bo et al. (PandaX), arXiv:2407.10892
3. First detection of coherent elastic neutrino-nucleus scattering on germanium, S. Adamski et al. (COHERENT), arXiv:2406.13806
4. Final CONUS results on coherent elastic neutrino-nucleus scattering at the Brokdorf reactor, N. Ackermann et al. (CONUS), arXiv:2401.07684
5. First results of the nuGeN experiment on coherent elastic neutrino-nucleus scattering, I. Alekseev et al. (nuGeN), Phys.Rev.D 106 (2022) L051101, arXiv:2205.04305.
6. Suggestive evidence for Coherent Elastic Neutrino-Nucleus Scattering from reactor antineutrinos, J. Colaresi, J.I. Collar, T.W. Hossbach, C.M. Lewis, K.M. Yocum, Phys.Rev.Lett. 129 (2022) 211802, arXiv:2202.09672
7. Search for coherent elastic neutrino-nucleus scattering at a nuclear reactor with CONNIE 2019 data, Alexis Aguilar-Arevalo et al. (CONNIE), JHEP 22 (2020) 017, arXiv:2110.13033
8. Measurement of the Coherent Elastic Neutrino-Nucleus Scattering Cross Section on CsI by COHERENT, D. Akimov et al. (COHERENT), Phys.Rev.Lett. 129 (2022) 081801, arXiv:2110.07730
9. First results from a search for coherent elastic neutrino-nucleus scattering (CEvNS) at a reactor site, J. Colaresi, J. I. Collar, T. W. Hossbach, A. R. L. Kavner, C. M. Lewis, A. E. Robinson, K. M. Yocum, Phys.Rev.D 104 (2021) 072003, arXiv:2108.02880
10. Search for coherent elastic scattering of solar 8B neutrinos in the XENON1T dark matter experiment, E. Aprile et al. (XENON), Phys.Rev.Lett. 126 (2021) 091301, arXiv:2012.02846
11. COHERENT Collaboration data release from the first detection of coherent elastic neutrino-nucleus scattering on argon, D. Akimov et al. (COHERENT), arXiv:2006.12659
12. First Detection of Coherent Elastic Neutrino-Nucleus Scattering on Argon, D. Akimov et al. (COHERENT), Phys.Rev.Lett. 126 (2021) 012002, arXiv:2003.10630
13. First Constraint on Coherent Elastic Neutrino-Nucleus Scattering in Argon, D. Akimov et al. (COHERENT), Phys.Rev. D100 (2019) 115020, arXiv:1909.05913
14. COHERENT Collaboration data release from the first observation of coherent elastic neutrino-nucleus scattering, D. Akimov et al. (COHERENT), arXiv:1804.09459
15. Observation of Coherent Elastic Neutrino-Nucleus Scattering, D. Akimov et al. (COHERENT), Science 357 (2017) 1123-1126, arXiv:1708.01294

CEvNS CROSS SECTION: STANDARD MODEL

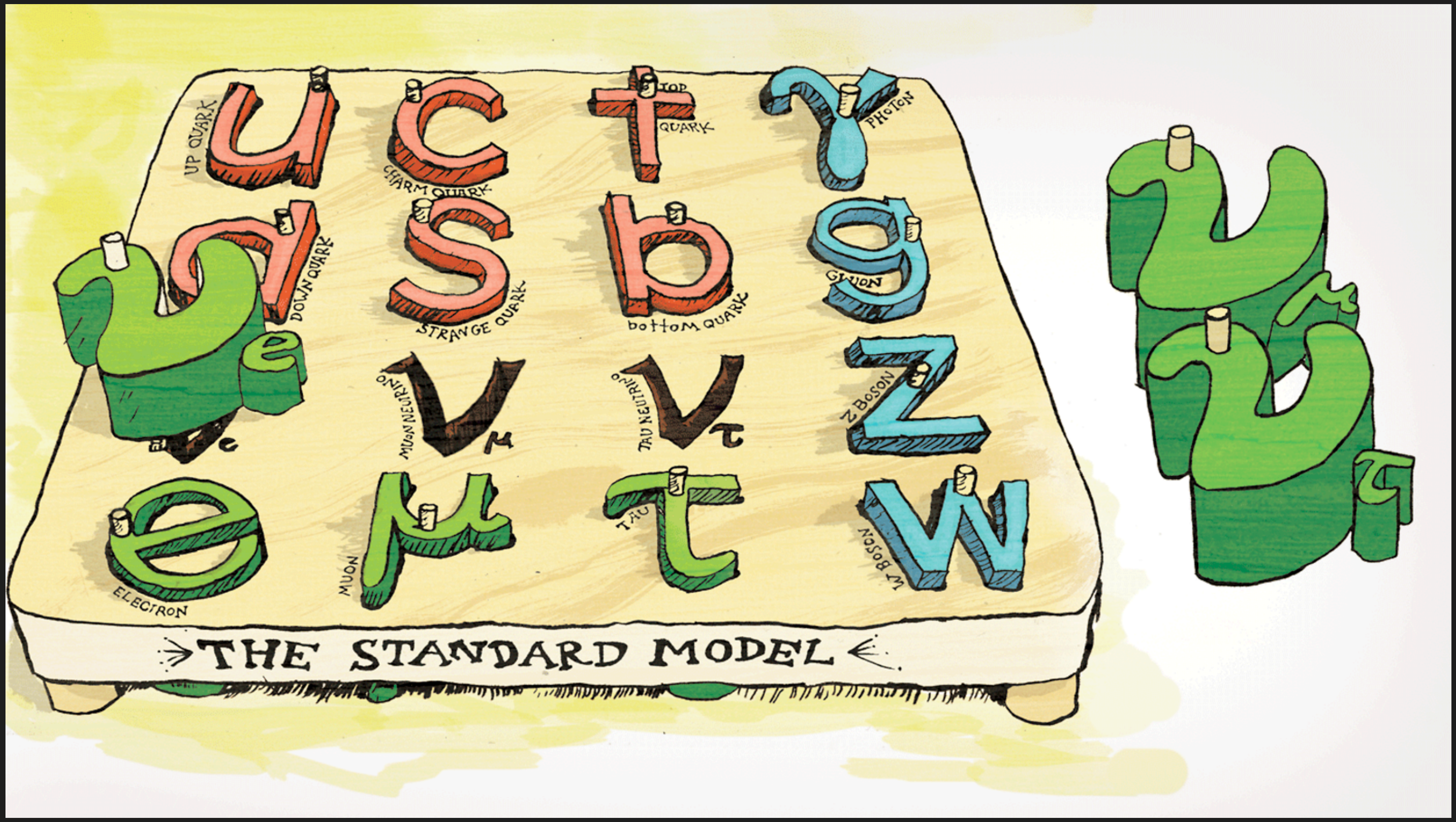

Illustration by Sandbox Studio, Chicago

CEνNS CROSS SECTION IN THE SM

Interplay of particle, hadronic and nuclear physics

$$\left.\frac{d\sigma_{\nu\mathcal{N}}}{dE_{\rm nr}}\right|^{\rm SM}_{\rm CE\nu NS} \propto \left|\sum_i c_i\ \mathrm{kin}_i\ \mathcal{F}_i\right|^2$$

Kin_i : kinematics terms

C_i: particle physics coefficients (coupling neutrino-quarks)

$\mathcal{F}_i$: nuclear structure physics

In the Donnelly-Walecka approach any semi-leptonic nuclear process at low and intermediate energies can be described by an effective interaction Hamiltonian, written in terms of the leptonic and hadronic currents

$$\langle \mathrm{final}\,|\,\mathscr{L}\,|\,\mathrm{initial}\rangle = \langle \mathrm{final}\,|\int d^3\mathbf{x}\ \hat{j}^{\rm lept}_{\mu}(\mathbf{x})\ \hat{J}^{\mu}(\mathbf{x})\,|\,\mathrm{initial}\rangle$$

The accurate evaluation of the required transition matrix elements is obtained on the basis of reliable nuclear wave functions.

CEνNS CROSS SECTION IN THE SM

We follow a multi-step process:

1. First, we define the effective neutrino-quark interaction in the non-relativistic limit (small momentum transfer) — same as going from the electroweak theory to the Fermi four-fermion theory
2. Second, we need to account for the quark content of the nucleons: we need to take the quark field operators and express them in terms of nucleon ones
3. Finally, we need to promote the operators at the nucleon level to the nuclear one. We need a nuclear model.

Freedman Phys. Rev. D 9, 1389-1392 (1974)
Drukier, Stodolsky, PRD 30 (1984) 2295
Amanik+ Astropart.Phys. 24 (2005) 160-182
J. Barranco+ JHEP 0512 (2005) 021
Papoulias+ Advances in High Energy Physics, vol. 2015, 763648
Lindner+ JHEP03(2017)097
Hoferichter+ Physical Review D 102, 074018 (2020)
Tomalak+ JHEP 2102, 097 (2021) (Radiative corrections)
Pandey Prog.Part.Nucl.Phys. (2023)
Khaleq+ arXiv:2405.20060

CEνNS CROSS SECTION IN THE SM

We want to compute the cross-section for the process $\nu_\ell \mathcal{N} \to \nu_\ell \mathcal{N}$.
Elastic process: final state nucleus remains unvaried.

The momentum transfer is much smaller than the mass of the mediator, so we can define an effective Lagrangian for the process.

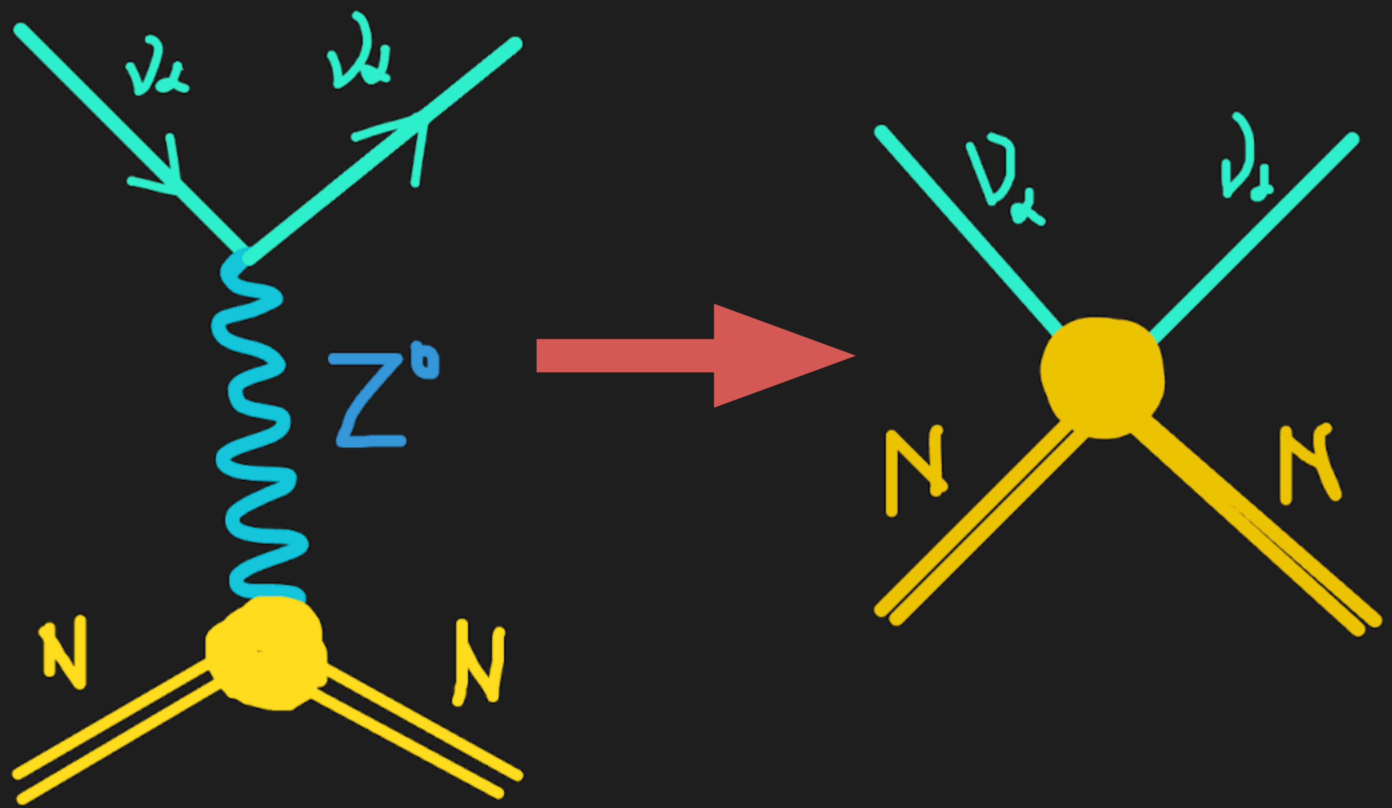

CEvNS CROSS SECTION IN THE SM

$$\mathscr{L}_{\text{eff}}^{\text{NC}} = \frac{\text{G}_\text{F}}{\sqrt{2}} \sum_q \left[\bar{\nu}\gamma^\mu(g_V^\nu - g_A^\nu\gamma^5)\nu\right] \left[\bar{q}\gamma_\mu(g_V^q - g_A^q\gamma^5)q\right]$$

The Lagrangian is defined as a sum of the interactions at the quark level.
The vector and axial couplings at the tree level are:

$$g_V^\nu = 1/2 \qquad g_A^\nu = 1/2$$

$$g_V^q = \boxed{T_3^q} - 2Q^q\sin^2\theta_\text{w} = \begin{cases} 1/2 - 1/3\sin^2\theta_\text{w} & \text{q = u,c,t} \\ -1/2 + 2/3\sin^2\theta_\text{w} & \text{q = d,s,b} \end{cases}$$

3rd component
Weak Isospin

The term $\bar{q}\gamma^\mu\gamma^5 q$ is the spin-dependent one. It is suppressed compared to the vector current. Only relevant for light nuclei with non-zero spin. Nuclei with even number of protons and neutrons have zero spin, so that axial terms vanish.

CEνNS CROSS SECTION IN THE SM

Promote the quark operators to the nucleon level.
Project the quark current on the initial and final nucleon states:

$$\langle \eta(p_f) | \mathcal{O}_q | \eta(p_i) \rangle = \langle \eta(p_f) | \bar{q}\gamma^\mu q | \eta(p_i) \rangle$$

$$= \bar{u}_N \left(\boxed{F_1^{q,\eta}(\mathbf{q}^2)\gamma^\mu} + F_2^{q,\eta}(\mathbf{q}^2) \frac{i\sigma^{\mu\nu} q_\nu}{2m_\eta} \gamma^\mu \right) u_N$$

The nucleon matrix element can be parametrized by means of its transformation properties under the Lorentz symmetry, spatial parity and time reversal. F_2 is suppressed (involves spin and goes as q/m_η). At zero momentum transfer, vector currents 'count' the valence quarks in the nucleon.

$$\sum_{\eta=n,p} \sum_q \langle g_V^q \eta(p_f) | \bar{q}\gamma^\mu q | \eta(p_i) \rangle$$

$$= \underbrace{\boxed{(g_V^u + 2g_V^d)}}_{g_V^p} \bar{n}\gamma^\mu n + \underbrace{\boxed{(2g_V^u + g_V^d)}}_{g_V^n} \bar{p}\gamma^\mu p$$

CEvNS CROSS SECTION IN THE SM

Final step: we need to go from interaction with nucleons to interaction with the nucleus.
At non-zero momentum transfer there will be a form-factor suppression given by the specific nuclear wave.
Construct the nuclear operator:

$$\langle \mathcal{N}(k_f) \,|\, \bar{\eta}\gamma^\mu\eta \,|\, \mathcal{N}(k_i)\rangle = \boxed{N_\eta}\, \bar{\mathcal{N}}\gamma^\mu\mathcal{N} F_{\mathrm{v}}^{\eta}(\mathbf{q}^2)$$

Counts nucleons inside nuclei

$$= \left[Z g_{\mathrm{v}}^{p} F_{\mathrm{v}}^{p}(\mathbf{q}^2) + N g_{\mathrm{v}}^{n} F_{\mathrm{v}}^{n}(\mathbf{q}^2)\right] \bar{\mathcal{N}}\gamma^\mu\mathcal{N}$$

The weak form factor is defined as

$$\tilde{F}_{\mathrm{W}}(\mathbf{q}^2) = \left[Z g_{\mathrm{v}}^{p} F_{\mathrm{v}}^{p}(\mathbf{q}^2) + N g_{\mathrm{v}}^{n} F_{\mathrm{v}}^{n}(\mathbf{q}^2)\right]$$

And then normalized to one through (valid at q $\rightarrow 0$)

$$Q_{\mathrm{W}} = (Z g_{\mathrm{v}}^{p} + N g_{\mathrm{v}}^{n}) = -N/2 + (1/2 - 2\sin^2\theta_{\mathrm{W}})Z$$

$$F_{\mathrm{W}}(\mathbf{q}^2) = \frac{\tilde{F}_{\mathrm{W}}(\mathbf{q}^2)}{Q_{\mathrm{W}}}$$

CEvNS CROSS SECTION IN THE SM

$$\mathscr{L}_{\rm eff}^{\rm NC} = \frac{\rm G_F}{\sqrt{2}} \sum_q \left[\bar{\nu}\gamma^\mu P_L \nu\right] \left[Q_{\rm w} F_{\rm w}(\mathbf{q}^2) \bar{\mathcal{N}} \gamma_\mu \mathcal{N}\right]$$

Assume the nucleus is in a fermionic ground state, we can compute the amplitude squared of the process, starting from the matrix element

$$\mathscr{M}^{ss'rr'} = \frac{\rm G_F}{\sqrt{2}} Q_{\rm w} F_{\rm w}(\mathbf{q}^2) \left[\bar{u}^{s'}(p')\gamma^\mu P_L u^s(p)\right] \left[\bar{u}^{r'}(k')\gamma_\mu u^r(k)\right]$$

$$|\mathscr{M}|^2 = \frac{\rm G_F^2}{4} Q_{\rm w}^2 F_{\rm w}^2(\mathbf{q}^2) L^{\mu\nu} W_{\mu\nu}$$

Lepton tensor ($L^{\mu\nu}$) — Hadron tensor ($W_{\mu\nu}$)

CEvNS CROSS SECTION IN THE SM

$$\left.\frac{d\sigma_{\nu\mathcal{N}}}{dE_{\rm nr}}\right|_{\rm CE\nu NS}^{\rm SM} = \frac{G_F^2 m_N}{128\pi}\frac{Q_{\rm w}^2 F_{\rm w}^2(\mathbf{q}^2)}{E_\nu^2 m_N} L^{\mu\nu}W_{\mu\nu}$$

Performing all traces calculations one obtains

$$\left.\frac{d\sigma_{\nu\mathcal{N}}}{dE_{\rm nr}}\right|_{\rm CE\nu NS}^{\rm SM} = \frac{G_F^2 m_N}{\pi} F_W^2(\mathbf{q}^2) Q_{\rm w}^2 \left(1 - \frac{m_N E_{\rm nr}}{2E_\nu^2} - \frac{E_{\rm nr}}{E_\nu} + \frac{E_{\rm nr}^2}{2E_\nu^2}\right)$$

$$Q_{\rm W} = -N/2 + (1/2 - 2\sin^2\theta_{\rm w})Z$$

$\sin^2\theta_w = 0.23$ → protons unimportant

Neutron contribution dominates

FORM FACTORS

The form factor corrects for scattering that is not completely coherent at higher energies.
It encodes information about the nuclear densities through a Fourier transform of the nuclear charge density distribution

$$F_{n,p}(q^2) = \frac{1}{Q_a}\int \rho_{p,n}(\vec{r})e^{i\vec{q}\cdot\vec{r}}d^3\vec{r}$$

Q_a is the charge of the entire distribution.
Assuming a spherically symmetrical distribution:

$$F_{n,p}(q^2) = \frac{4\pi}{Q_a q}\int \rho_{p,n}(r)\sin(q\cdot r)rdr$$

Patton et al, arXiv:1207.0693
Bednyakov, Naumov, arXiv:1806.08768
Papoulias et al, Phys.Lett. B800 (2020) 135133
Ciuffoli et al, arXiv:1801.02166
Canas et al, arXiv:1911.09831
Van Dessel et al, arXiv:2007.03658
Aristizabal-Sierra JHEP 1906:141 (2019)
Coloma+ JHEP 08 (2020) 08, 030
Aristizabal-Sierra Phys.Lett.B 845 (2023) 138140

FORM FACTORS

We can expand the form factor in terms of q:

$$F_{n,p}(q^2) \approx \int \rho_{p,n}(r)\left(1 - \frac{q^2}{3!}r^2 + \frac{q^4}{5!}r^4 - \frac{q^6}{7!}r^6 + \ldots\right) r^2 dr$$

$$\approx 1 - \frac{q^2}{3!}\langle R^2_{p,n}\rangle + \frac{q^4}{5!}\langle R^4_{p,n}\rangle - \frac{q^6}{7!}\langle R^6_{p,n}\rangle + \ldots$$

with the k-th radial moment defined as

Patton et al, arXiv:1207.0693
Papoulias et al, Phys.Lett. B800 (2020) 135133

$$\langle R^k_{p,n}\rangle = \frac{\int \rho_{p,n}(\vec{r}) r^k d^3\vec{r}}{\int \rho_{p,n}(\vec{r}) d^3\vec{r}}$$

In this way the form factor is a sum of the even moments of the neutron density distribution, that represent physically relevant and measurable quantities.

FORM FACTORS

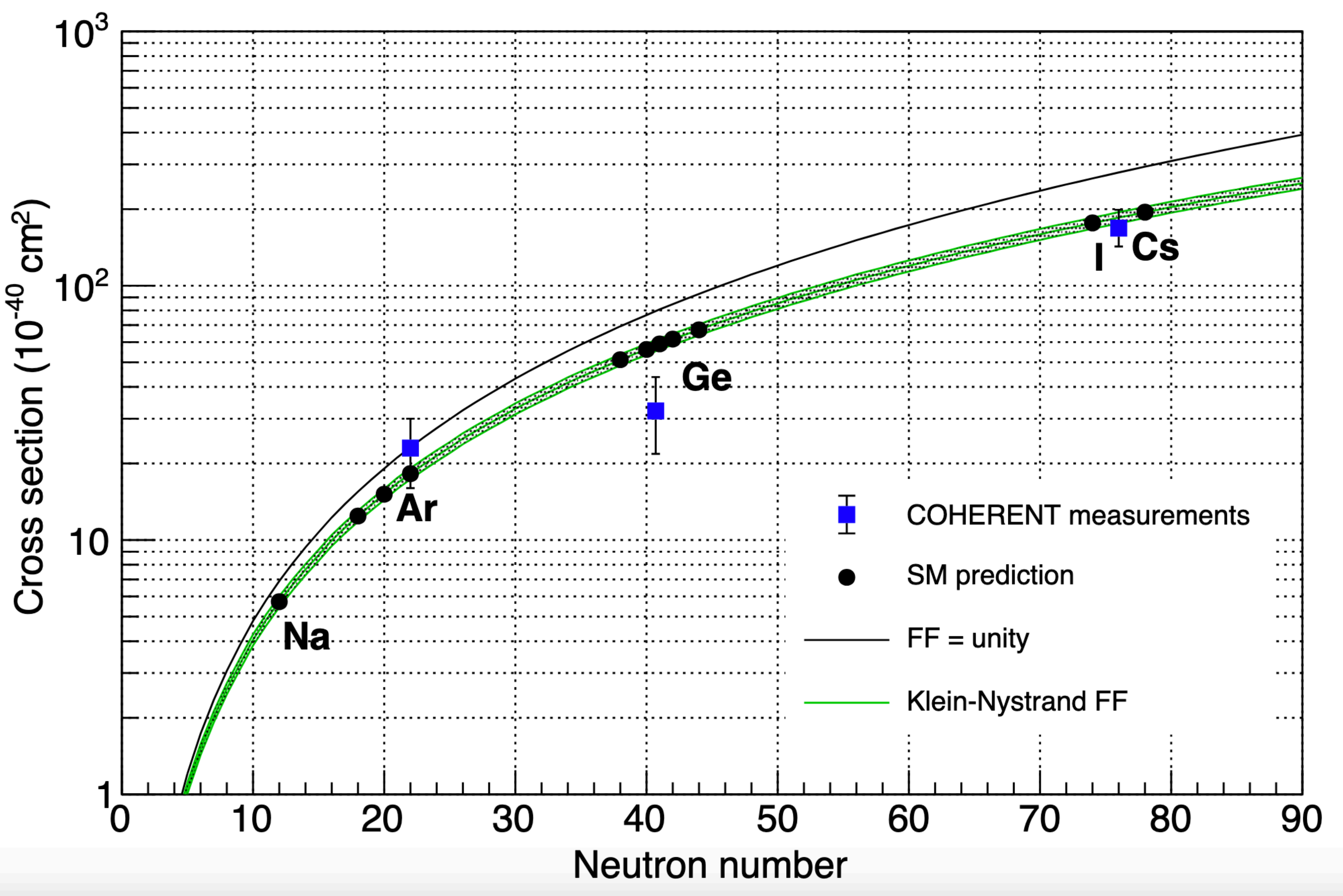

From Ryan Bouabid's talk @Magnificent CEvNS2024

FORM FACTORS

How to obtain the nuclear form factors:

- Nuclear structure calculations; S. Kosmas+ Nucl. Phys. A 570 (1994) 637
  Papoulias+ Phys.Lett. B800 (2020) 135133

- Use of available experimental data: the proton nuclear form factors are computed by means of a model-independent analysis (using a Fourier-Bessel expansion model or others) of the electron scattering data for the proton charge density; De Vries+ Data and Nucl. Data Tables 36 (1987) 495536

- Use of analytical approximations for the nuclear form factors.

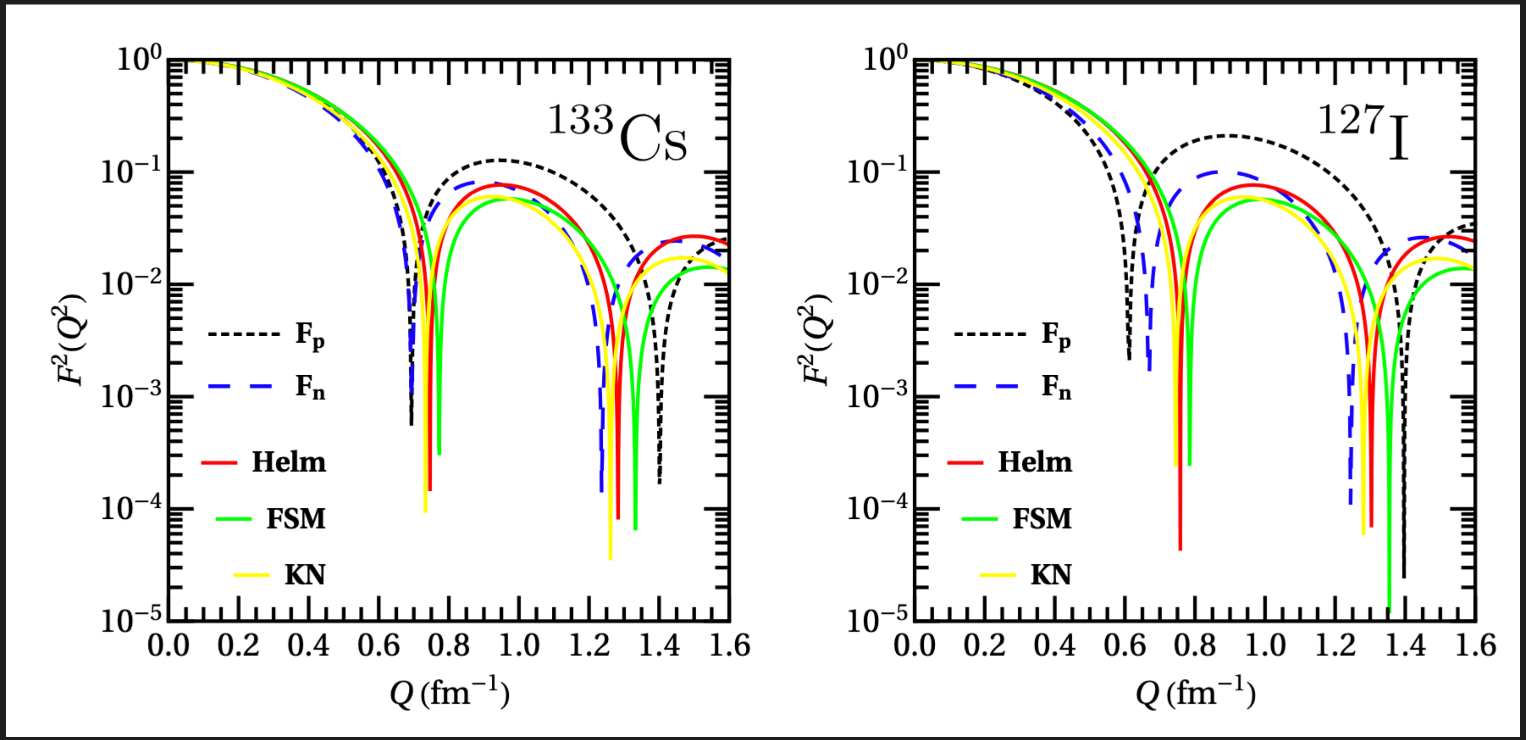

Papoulias+ Phys.Lett. B800 (2020) 135133

FORM FACTORS: PARAMETRIZATIONS

The basic properties of nucleonic distributions can be described by different parametrizations.

J. Engel, Phys.Lett. B 264 (1991) 114

In the Helm model, the nuclear form factor is given by the convolution of two nucleonic densities: a uniform-density one with a cut-off radius R_0 and a second one with a Gaussian profile, in terms of the surface thickness s.

$$F_{\mathrm{Helm}}(q^2) = 3\frac{j_1(qR_0)}{qR_0}e^{(-qs)^2/2}$$

Helm Phys. Rev. 104 (1956) 1466–1475

$j_1(x)$ denotes the 1st-order spherical Bessel function.

The root-mean-square (rms) radius $\langle R_n^2 \rangle = \frac{3}{5}R_0^2 + 3s^2$

s = 0.9 from muon spectroscopy data Fricke Nucl.Data Tabl. 60 (1995) 177–285

FORM FACTORS: PARAMETRIZATIONS

The Klein-Nystrand form factor follows from the convolution of short-range Yukawa potential with $a_k = 0.7$ fm, over a distribution approximated as a hard sphere with radius R_a.

$$F_{\mathrm{KN}}(q^2) = 3\frac{j_1(qR_A)}{qR_A}\left[1 + (qa_k)^2\right]^{-1}$$

Klein, Nystrand Phys. Rev. C60 (1999) 014903

$j_1(x)$ denotes the 1st-order spherical Bessel function.

The root-mean-square (rms) radius $\langle R_n^2 \rangle = \frac{3}{5}R_A^2 + 6a_k^2$

semi-empirical formula

$$R_A \approx 1.2 \times A^{1/3}\mathrm{fm}$$

NUCLEAR RMS RADIUS

The form factor parametrizations depend on two parameters that measure different nuclear properties and that are constrained by means of the rms radius of the distribution:

$$\langle R^2_{p,n} \rangle = \frac{\int \rho_{p,n}(\vec{r}) r^2 d^3\vec{r}}{\int \rho_{p,n}(\vec{r}) d^3\vec{r}}$$

The rms radii of the proton density distributions are determined from different experimental sources: optical and X-ray isotope shifts, muonic spectra, and electronic scattering experiments.

Angeli+ Atom. Data Nucl. Data Tabl. 99, 69 (2013)

Neutron rms radii: their experimental values follow from hadronic experiments which are subject to large uncertainties.

CEνNS CROSS SECTION: RECAP

CEνNS has a well-calculable cross-section in the SM:
(probability of kicking a nucleus with nuclear recoil energy T)

Fermi constant (SM parameter)

Kinematics

Nuclear Form Factor: F=1 full coherence

$$\frac{d\sigma}{dT} = \frac{G_F^2 M}{4\pi}\left(1 - \frac{MT}{2E_\nu^2} - \frac{T}{E_\nu}\right)Q_w^2\left[F_w(q^2)\right]^2 + \frac{G_F^2 M}{4\pi}\left(1 + \frac{MT}{2E_\nu^2} - \frac{T}{E_\nu}\right)F_A(q^2)$$

Weak nuclear charge

$$Q_W = [Z(1 - 4\sin^2\theta_W) - N]$$

$s_W^2 = 0.23$ → protons unimportant
Neutron contribution dominates

- E_ν: is the incident neutrino energy
- M : the nuclear mass of the detector material
- 3-momentum transfer $|\vec{q}|^2 = 2MT$
- (Q_A included in F_A)

Axial contribution is small for most nuclei, spin-dependent.
It vanishes for nuclei with even number of protons and neutrons

Freedman, PRD 9 (1974) 1389; Drukier, Stodolsky, PRD 30 (1984) 2295; Barranco, Miranda, Rashba, hep-ph/0508299